Technische Universität München

Kinderklinik und Poliklinik der TU München

Children´s Cancer Research Center

Univ.-Prof. Dr. St. Burdach

THE ROLE OF MONDOA IN CHILDHOOD LEUKEMIA

Caroline Magdalena Wernicke

Vollständiger Abdruck der von der Fakultät für Medizin der Technischen Universität München zur Erlangung des akademischen Grades eines Doktors der Medizin genehmigten Dissertation.

Vorsitzender: Univ.- Prof. Dr. E. J. Rummeny

Prüfer der Dissertation:

           1. Univ.- Prof. Dr. St. Burdach

           2. apl. Prof. Dr. G. Keller

           3. Univ.- Prof. Dr. A. Krackhardt

Die Dissertation wurde am 19.12.2013 bei der Technischen Universität München eingereicht und durch die Fakultät für Medizin am 17.12.2014 angenommen.

Content

Abbreviations

ABL1	Abelson tyrosine-protein kinase 1
APC	Allophycocyanin
AIEOP-BFM ALL 2000	Associazione Italiana di Ematologia Oncologia Pediatrica and the Berlin-Frankfurt-Münster Acute Lymphoblastic Leukemia
ALL	acute lymphoblastic leukemia
bHLHZip	basic helix-loop-helix leucine zipper
BM	bone marrow
Bp	base pairs
BrdU	Bromodeoxyuridine
B2M	beta-2-microglobulin
cALL	common acute lymphoblastic leukemia
CD	cluster of differentiation
cDNA	complementary DNA
CI	confidence interval
CRM1	exportin 1
DDIT3	DNA-damage-inducible transcript 3
DNA	desoxyribonucleic acid
DNTT	deoxynucleotidyltransferase, terminal
EGIL	European Group for the Immunological Characterization of Leukemias
FC	fold change
FEB	fetal early B cells
FITC	fluorescein isothiocyanate
GPOH	Society for Pediatric Oncology and Hematology
GSEA	gene-set enrichment analysis
Gluc	glucose
HLA-DR	human leukocyte antigen -DR
H&E	hematoxylin and eosin
Inv	inventoried
kDa	kiloDalton

MCR	MondoA conserved region
MEFs	mouse embryonic fibroblasts
MLX	MAX-like-protein
MlxH	dimerization with MLX cytoplasmatic retention domain
MLXIPL	MAX-like interacting protein-like, also known as MondoB
MRD	Minimal Residual Disease
Mto	made-to-order
NES	normalized enrichment score
NOD-SCID	non - obese diabetic - severe combined immunodeficiency
NTC	non-template control
PBMCs	peripheral blood mononuclear cells
PCR	polymerase chain reaction
PDGFRA	platelet-derived growth factor receptor alpha
PE	R-Phycoerythrin
PI	propidium iodide
pSImondoA	stably MondoA silenced Nalm6 cells
pSInegative	non-silenced Nalm6 cells
qRT-PCR	quantitative real-time PCR
$r_{Spearman}$	Spearman's rank correlation coefficient
RNA	ribonucleic acid
RNAi	RNA interference
RUNX1	runt-related transcription factor 1, also known as AML1
SAM	significance analysis of microarrays
SEM	standard error of the mean
shRNA	short hairpin RNA
siRNA	small interfering RNA
TAD	Transcriptional activation domain
TF	transcription factor
TGFBR2	transforming growth factor beta receptor 2
TSS	transcriptional start site

TXNIP	thioredoxin interacting protein
WBC	white blood cell count
7-AAD	7-aminoactinomycin-D

1 Introduction and objectives

1.1 Acute lymphoblastic leukemia

1.1.1 Terminology and nosology:

Leukemia (from greek: leukós >white< and haima >blood<) are malignant diseases of the hematopoietic system. Acute and chronic clinical courses can be distinguished. Acute leukemia are divided into lymphoblastic and myeloid leukemia, originating from the lymphoid or the myeloid line in the hematopoiesis, respectively. Lymphoblastic leukemia can be further divided into B and T cell leukemia depending on their differentiation into the B or T lineage from a common lymphoid progenitor.

Acute lymphoblastic leukemia (ALL) is the most common childhood cancer, which is generally associated with good overall survival rates of around 80% (Pui et al., 2011). The cumulative risk of any child developing leukemia before the age of 15 years is around 1 in 2,000 (Greaves and Wiemels, 2003; Pui et al., 2011). Common ALL (cALL) is the most frequent entity of childhood ALL, carries an early pre-B cell phenotype (**Figure 1**) and has a marked age-incidence peak at 2-5 years and a boys/girls ratio of 1.2/1 (Eden, 2010). 15 years ago, the two most important factors predictive of outcome were age and white blood cell count (WBC) reflective of tumor burden at diagnosis, with age > 10 years and WBC > 50,000/µL as higher risk groups (Smith et al., 1996). Recently, the Associazione Italiana di Ematologia Oncologia Pediatrica and the Berlin-Frankfurt-Münster Acute Lymphoblastic Leukemia (AIEOP-BFM ALL 2000) study found that Minimal Residual Disease (MRD) discriminated prognosis even on top of white blood cell count, age, early response to prednisone, and genotype (Conter et al., 2010).

1.1.2 Current concepts of leukemogenesis:

ALL is a biologically heterogeneous disease and no single or exclusive causal mechanism is likely to account for all types of ALL (Greaves, 2006). Like other tumors, ALL results from the accumulation of somatic abnormalities that affect normal control of cellular growth (Pui et al., 2008). For instance, chromosome translocations are often early or initiating events in leukemogenesis, occurring prenatally in most cases of childhood leukemia (Greaves, 2006). For instance, genetic lesions such as the TEL-AML fusion were found in the blood of up to 75% of neonatals that will develop ALL up to 14 years of age (Gale et al., 1997; Wiemels et al., 1999a, 1999b). Furthermore, inactivation of tumor suppressor genes is a critical step in leukemogenesis of ALL. Besides, DNA methylation at CpG sites in the promoter region can cause gene silencing, which may provide an alternate modus of gene inactivation in addition to their deletions or mutations. Methylation in the promoter region is a frequent, acquired epigenetic event involved in the pathogenesis of many human malignancies including leukemia (Uehara et al., 2003; Taylor et al., 2007; Kuang et al., 2008). An abnormal immune response to common infections as a trigger for leukemia is also discussed, but the mechanisms remain to be determined (Kinlen, 1988; McNally and Eden, 2004; Greaves, 2006).

1.1.3 Symptoms of ALL:

Clinical signs are often unspecific with general fatigue, petechiae, fever and frequent infections resulting from pancytopenia as the normal hematopoiesis in the bone marrow is suppressed by the fast expanding leukemic blasts. The resulting anemia causes pallor, dyspnea and fatigue, the thrombocytopenia facilitates bleeding and bruising and the neutropenia leads to immunosuppression with frequent infections (Margolin JF et al.). Hepatosplenomegaly and lymphadenopathy are seen in two

thirds of the patients (Margolin JF et al.). Bone pain, particularly affecting the long bones, and caused by leukemic involvement of the periostium, is a presenting symptom in one third of cases (Sinigaglia et al., 2008). Leukemia cells can also spread to the central nervous system and cause headache, vomiting, lethargy, nuchal rigidity and rarely cranial nerve abnormalities (Bleyer, 1988; Ingram et al., 1991).

1.1.4 Diagnosis of ALL:

In addition to clinical signs of pancytopenia, blasts in smears of peripheral blood and more than 25% blasts in the bone marrow aspirate (**Figure 1**) (Brunning RD et al.), a variety of laboratory studies including morphology, immunophenotyping, cytogenetics and molecular diagnostics are performed to establish the diagnosis and assign patients to specific risk groups (Carroll et al., 2003; Pui et al., 2011).
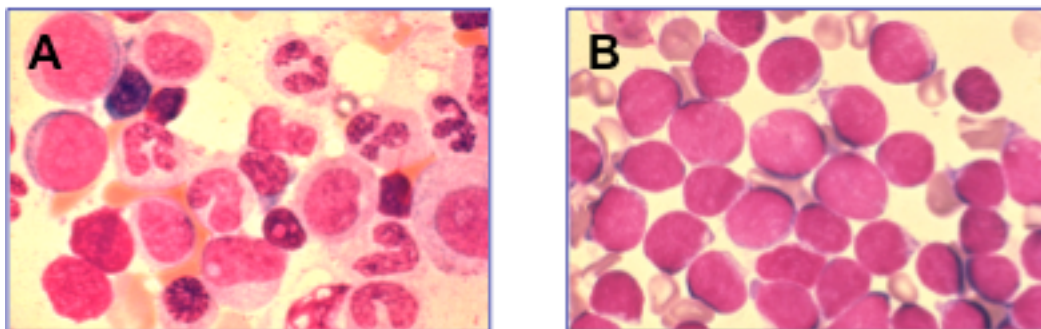
Figure 1 – representative images of bone marrow aspirates of healthy and cALL bone marrow
(A) pleiomorphic cells of healthy bone marrow
(B) pleiomorphic cells of healthy bone marrow have been replaced by monomorphic cALL cells in the cALL bone marrow

These images were derived from the Atlas of Hematology, Nagayo University School of Medicine, http://pathy.med.nagoya-u.ac.jp (with permission of the authors and the publisher tsuzaka@met.nagoya-u.ac.jp)

1.1.4.1 B cell differentiation and immunophenotypic characterization:

B cell maturation starting from a lymphoid progenitor cell takes entirely place in the bone marrow. Mature B cells enter the circulation and migrate to the peripheral lymphoid organs, where they differentiate into antibody secreting plasma cells upon activation by antigens (Murphy et al.)(Janeway CA, Immunobiology, 2001).

The stages of B cell maturation are characterized by a specific pattern of membrane proteins that act as phenotypic markers of these developmental stages, which can be detected by flow cytometry and are used to assign leukemic blasts to a specific subtype of leukemia (Murphy et al.) (Janeway CA, Immunobiology, 2001).

Common ALL in children are defined as CD45+, HLA-DR+, CD19+, CD79a+, CD10+ and $CD22_Z$+ after the European Group for the Immunological Characterization of Leukemias (EGIL) (**Figure 2**).
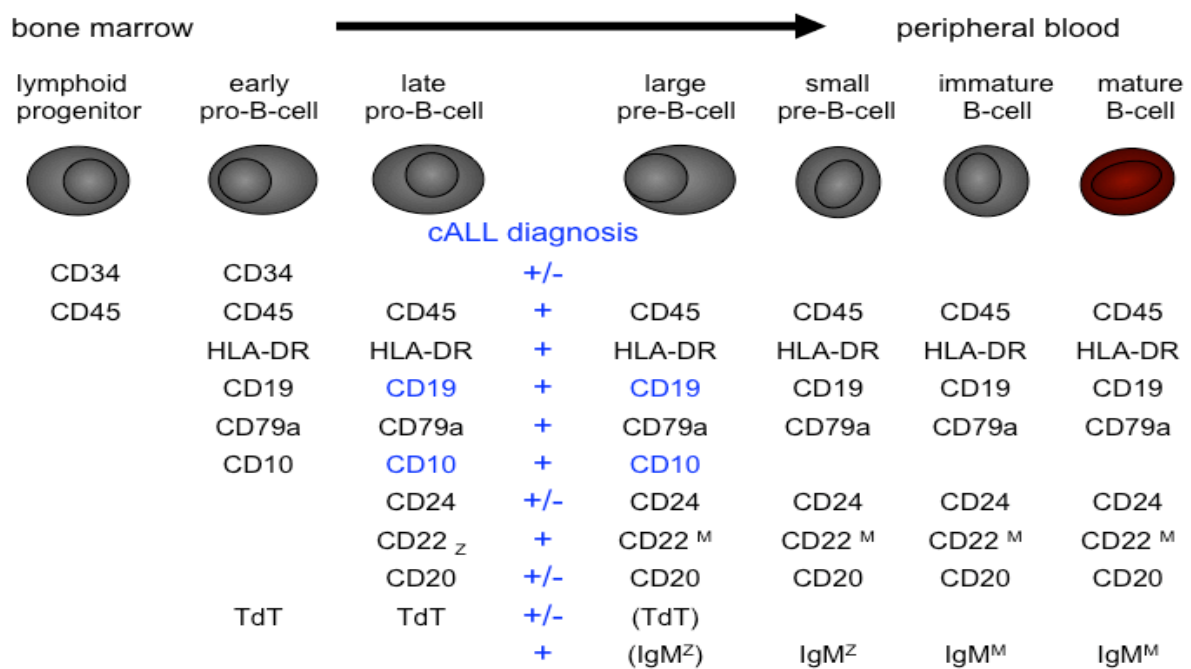
Figure 2 - B-cell maturation stages with examples of immunophenotypic markers expressed in the normal development of these cells. Z: cytoplasm, M: membrane

The depicted image was modified from Janeway CA et al., Immunobiology (Churchill Livingstone), 2001 (Murphy et al.).

1.1.5 Current concepts of treatment of ALL:

Controlled clinical trials of chemotherapy and the development of protocols that include optimized chemotherapy combinations, effective central nervous system prophylaxis, post-induction intensification of therapy, and a prolonged maintenance phase of treatment have steadily improved the survival of children with acute leukemia to the current figure of around 80% (Pui et al., 2011). Stratification of patients into therapy regimens of different intensity is based on the individual risk for relapse by using prognostic factors including cytogenetics and response to therapy to define different risk groups (Schrappe et al., 2000; Silverman and Sallan, 2003; Pui and Evans, 2006). High-risk patients are candidates for intensified therapy including allogeneic hematopoietic stem cell transplantation in first remission, while those with low-risk features may be candidates for less aggressive therapy (Carroll et al., 2003; Silverman and Sallan, 2003; Pui and Evans, 2006). Current protocols take at least two years and generally consist of four phases: induction, consolidation, reintensification, and maintenance (Möricke et al., 2010; Pui et al., 2011).

Glucocorticoids such as prednisone and dexamethasone have been used extensively in the treatment of childhood ALL for many years (Gaynon and Carrel, 1999). The in-vivo prednisone response has been shown to correlate with long-term clinical outcome in children with ALL (Kaspers et al., 1998; Lauten et al., 2001). In addition, L-Asparaginase and Vincristine are mainly used during induction and reintensification, while consolidation and maintenance are conducted with antimetabolites as 6-mercaptopurine and methotrexate (Möricke et al., 2010).

However, conventional therapies are accompanied by considerable short- and long-term toxicity (Bürger et al., 2005; Bourquin and Izraeli, 2010). Therefore, the development of targeted therapies may be the prerequisite to reduce the toxic burden of cure (Carroll et al., 2003; Bourquin and Izraeli, 2010).

1.2 The transcription factor MondoA

In order to identify potential targets for the treatment of cALL, a transcriptome analysis of early pre-B cell ALL and fetal early pre-B cells (FEB) was previously performed by Richter et al. that revealed a novel signature of genes specifically and/or highly overexpressed in ALL (Richter et al., 2005). This signature comprised 270 genes of which 40 (14.8%) are involved in cellular metabolism (Richter et al., 2005). One of the most prominent among them was MondoA (also known as MAX-like interacting protein, MLXIP) – the founding member of the basic helix-loop-helix leucine zipper (bHLHZip) transcription factors of the Mondo family, which have pleiotropic, but functionally largely uncharacterized effects on cell metabolism (Billin et al., 2000).

The MondoA gene on chromosome 12q24.31 encodes a protein of 911 amino acids (apparent molecular weight 101 kDa), which is ubiquitously expressed at low levels, but highly expressed in skeletal muscle (Billin et al., 2000). Its paralog, *MondoB* (also known as MAX-like interacting protein-like, *MLXIPL*), shows highest expression in the liver (Iizuka et al., 2004; Ishii et al., 2004), where it plays a role in regulation of aerobic glycolysis, *de novo* lipogenesis and nucleotide synthesis (Ma et al., 2005; Tong et al., 2009). The N-termini of MondoA and MondoB are conserved across family members and contain cytoplasmic localization and transcription activation domains (Billin et al., 2000; Tong et al., 2009). MondoA forms heterodimers with MAX-like-protein (MLX), a member of the MYC/MAX/MAD family of transcription factors (Billin et al., 2000; Billin and Ayer, 2006; Sans et al., 2006; Stoltzman et al., 2008) via dimerization with its MLX cytoplasmic retention domain (Eilers et al., 2002). This heterodimerization of MondoA and MLX seems to be essential for MondoA to exert its transcriptional function (Billin et al., 2000). Recently, MondoA:MLX heterodimers have been discussed as a parallel network to MYC:MAX heterodimers,

which are both oncogenes having broad effects on cellular growth, proliferation and survival (Kaadige et al., 2010; Sloan and Ayer, 2010). MondoA:MLX heterodimers localize to the outer mitochondrial membrane, the primary site of oxidative phosphorylation, where they are believed to sense changes in the intracellular energy state as they may accumulate in the nucleus upon excess glucose availability to guide an adaptive transcriptional response (Stoltzman et al., 2008). A two-step process is required for intranuclear accumulation and gene transcription. First, heterodimerization of MondoA:MLX abolishes cytoplasmic retention. Then, the nuclear export mediated by Exportin 1 (CRM1) and 14-3-3 binding to the MondoA conserved region (MCR) ll and lll at the N-terminus must be inactivated by extracellular signals (Eilers et al., 2002) (**Figure 3**). By this means, shuttle proteins such as MondoA transduce signals from the cell´s periphery to the nuclear transcriptional machinery. However, the integrity of these signaling pathways is often disrupted in cancer (Grunewald et al., 2009).

Figure 3 – functional structure of MondoA
(MCR) MondoA conserved region, (TAD) Transcriptional activation domain, (bHLHZip) basic helix-loop-helix leucine zipper, (MlxH) dimerization with MLX cytoplasmic retention domain

Current data suggest that MondoA coordinates the utilization of glucose and glutamine by regulating the expression of thioredoxin interacting protein (TXNIP) (Stoltzman et al., 2008; Kaadige et al., 2009; Peterson and Ayer, 2012). TXNIP interacts with thioredoxin, resulting in elevated reactive oxygen species levels and

increased apoptosis (Muoio, 2007). Furthermore, TXNIP is considered as a tumor suppressor as its overexpression causes cell cycle arrest and its levels are reduced in tumors (Goldberg et al., 2003; Han et al., 2003). Consistent with these findings, high TXNIP expression portends a positive outcome in breast and gastric cancers (Cadenas et al., 2010; Chen et al., 2010). Besides, studies strongly implicate TXNIP as a negative regulator of glucose uptake and aerobic glycolysis (Hui et al., 2008; Shin et al., 2008). In the presence of glucose but absence of glutamine, MondoA induces TXNIP and thus restricts glucose uptake and cell proliferation (Stoltzman et al., 2008). Under physiological conditions, thus in the presence of both glucose and glutamine, MondoA represses TXNIP, resulting in a stimulation of glucose uptake (Kaadige et al., 2009). Glutamine inhibits transcriptional activation of TXNIP apparently by triggering the recruitment of a corepressor to the amino-terminus of MondoA (Kaadige et al., 2009).

Interestingly, also MondoB has been shown to stimulate cell growth and aerobic glycolysis in a colon cancer cell line (Tong et al., 2009).

1.3 Tumor metabolism and Warburg effect:

A near-universal metabolic feature of cancer cells is their preferential use of aerobic glycolysis. First observed by Otto Warburg in the 1920s, this glucose catabolism to lactate under aerobic conditions called Warburg´s effect has been widely investigated (WARBURG, 1956) (**Figure 4**). Mitochondrial uncoupling and abrogation of glucose sensing have been shown to lead to aerobic glycolysis seen in fast-growing tumor cells (WARBURG, 1956; Samudio et al., 2008, 2009). At a first glance, Warburg´s effect appears energetically inefficient, but emerging evidence suggests a considerable contribution to tumor initiation, survival and stemness. Warburg´s effect

8

fuels cancer cells with precursors required for their high levels of nucleotide and lipid biosynthesis during runaway proliferation (Vander Heiden et al., 2009).

As MondoA has been suggested as a sensor for intracellular energy state (Sans et al., 2006) and is highly expressed in leukemia, the author of this dissertation aimed to investigate a possible contribution of MondoA to Warburg´s effect in leukemia.
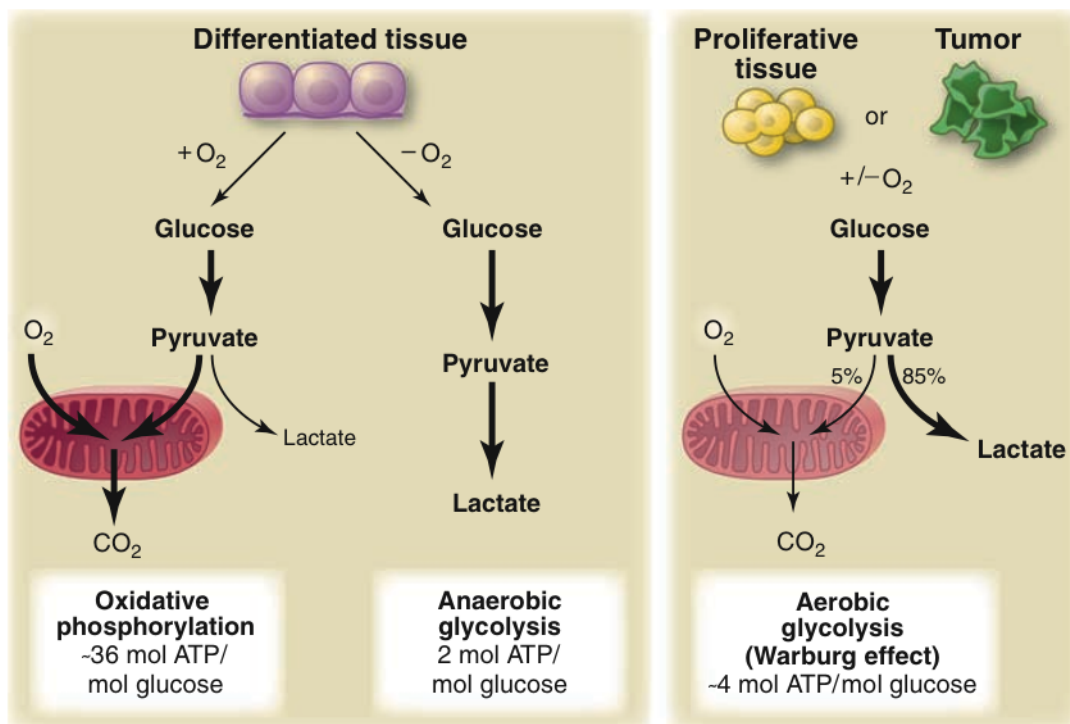
Figure 4 – Glycolysis in differentiated and malignant tissue
Van der Heiden MG et al., Science 2009 (Vander Heiden et al., 2009)

Based on these data, a modulation of the metabolic activity and a promotion of the proglycolytic phenotype by MondoA were hypothesized. The objectives of the current work were to verify the preliminary microarray data, to determine possible mechanisms of MondoA regulation and to define the functional role of MondoA in leukemia cells concerning glucose metabolism, survival and differentiation, thus to investigate its potential functional role for the malignant phenotype of ALL.

2 Materials and Methods

2.1 Materials

2.1.1 Human cell lines

Human T cell lineage ALL lines LOUCY, HSB-2, DND41, PEER, KE-37, ALL-SIL, HPB-ALL, ICHIKAWA, JURKAT-J6, MOLT-4, TALL1, JURKAT, BE13, and CCRF-CEM, as well as human B cell lineage ALL lines SKW6, cALL2, 697, SD-1 RS4;11, REH, and Nalm6 were obtained from the German Collection of Microorganisms and Cell Cultures (DSMZ) or ATCC (LGC standards), respectively. Hepatocellular carcinoma cell lines Hep3B and Hep2G were kindly provided by Prof. Dr. Elke Butt (Institute for Clinical Biochemistry, University of Würzburg, Germany). Retrovirus packaging cell line PT67 was obtained from Takara Bio Europe/Clontech (Saint-Germain-en-Laye, France).

2.1.2 Human samples

The Institutional Review Boards of the Universities of Halle-Wittenberg and Leipzig and the Technische Universität München approved the current study. Patient-derived ALL samples and cell preparations of blood of healthy donors [fetal early pre-B cells (FEB); peripheral blood mononuclear cells (PBMCs)] were obtained from the Departments of Pediatrics of the Universities of Halle-Wittenberg and Leipzig and the Technische Universität München according to legal guidelines of local authorities. Written informed consent was obtained from all donors and/or their legal guardians (Uwe E. Hattenhorst, 2003; Beate Beinvogl, 2010).

2.1.3 Cell culture media

RPMI 1640	Invitrogen, Karlsruhe, Germany
DMEM (Dulbecco´s modified Eagle medium)	Life Technologies, Karlsruhe, Germany

2.1.4 General material

Cryovials	Nunc, Naperville, IL, USA
Culture dishes (Nunclon™ Surface 100 mm)	Nunc, Naperville, IL, USA
Culture test plates (6- and 96- well)	TPP, Trasadingen, Switzerland
Gloves (nitrile and latex)	Sempermed, Vienna, Austria
Pipettes (5, 10, and 25 mL)	Falcon, Oxnard, CA, USA
Pipette tips (10, 200 and 1000 µL)	MbP, San Diego, CA, USA
Pipette tips with filter (10, 200 and 1000 µL)	Biozym, Hessisch Olendorf, Germany
Safe-lock tubes (0.5 and 1.5 mL)	Eppendorf, Hamburg, Germany
Syringe filters (0.2 and 0.45 µm)	Sartorius, Göttingen, Germany
Tissue culture flasks (75 and 175 cm^2)	Falcon, Oxnard, CA, USA
Tubes for cell culture (15 and 50 mL)	Falcon, Oxnard, CA, USA
Tubes for FACS TM (5 mL)	Falcon, Oxnard, CA, USA

2.1.5 Chemical and biological reagents

Diethyl pyrocarbonate (DEPC)	Sigma, Deisenhofen, Germany
Dimethyl sulfoxide (DMSO)	Merck, Darmstadt, Germany
Ethylenediaminetetraacetic acid (EDTA)	Merck, Darmstadt, Germany
Ethanol	Merck, Darmstadt, Germany
Fetal bovine serum (FBS)	Biochrom, Berlin, Germany
Gentamycin	Invitrogen, Karlsruhe, Germany
HiPerFect Transfection Reagent	Qiagen, Chatsworth, CA, USA
L- glutamine	Invitrogen, Karlsruhe, Germany
10 x Phosphate buffered saline (PBS)	Invitrogen, Karlsruhe, Germany
Polybrene	Sigma, Deisenhofen, Germany
Propidium iodide (PI)	Sigma, Deisenhofen, Germany
Puromycin	Sigma, Deisenhofen, Germany
TaqMan Universal PCR Master Mix	Applied Biosystems, Darmstadt, Germany
Zebularine	Sigma, Deisenhofen, Germany

2.1.6 Commercial reagent kits and assays

Absolute IDQ- Kit	Biocrates Life Sciences AG, Innsbruck, Austria
Amaxa® Cell Line Nucleofector® Kit L	Lonza, Basel, Switzerland

Annexin V-PE Apoptose Detection Kit I	BD Biosciences, Heidelberg, Germany
Cell proliferation ELISA BrdU Kit	Roche, Mannheim, Germany
Colony-forming assay	R&D Systems, Wiesbaden-Nordenstadt, Germany
GeneChip Whole Transcript Sense Target Labeling Kit	Affymetrix, Santa Clara, USA
High-Capacity cDNA Reverse Transcription Kit	Applied Biosystems, Darmstadt, Germany
iView DAB detection kit	Ventana Medical system, Roche, Mannheim, Germany
RNeasy® Mini Kit	Qiagen, Chatsworth, CA, USA
TaqMan® Gene Expression Assays	Applied Biosystems, Darmstadt, Germany
MycoAlert® Mycoplasma Detection Kit	Lonza, Basel, Switzerland

2.1.7 Instruments and equipment

Device	Name	Manufacturer
Balance	EW3000-2M	Kern, Balingen, Germany
Centrifuge	Multifuge 3 S-R	Heraeus, Hanau, Germany
Centrifuge	Biofuge fresco	Heraeus, Hanau, Germany

CD19 DETACHaBEADS		Invitrogen, Karlsruhe, Germany
CD19 Dynabeads		Dynal Biotech, Oslo, Norway
Electroporator	Amaxa® Nucleofector® I Device	Lonza, Basel, Switzerland
ELISA Reader	Multiscan Ascent	Thermo Fisher Scientific, Dreieich, Germany
Flow cytometer	FACSCalibur™	Becton Dickinson, New Jersey, NJ, USA
Freezer (- 80°C)	Hera freeze	Heraeus, Hanau, Germany
Freezer (- 20°C)	Cool vario	Siemens, Munich, Germany
Freezing container	Mr. Frosti	Nalgene, Rochester, NY, USA
Fridge (4°C)	Cool vario	Siemens, Munich, Germany
Glucometer	Breeze 2®	Bayer Vital GmbH, Leverkusen, Germany
Heating block	Thermomixer Comfort	Eppendorf, Hamburg, Germany
Hemocytometer	Neubauer	Brand, Wertheim,

		Germany
Ice machine	AF 100	Scotsman, Milan, Italy
Incubator	HERAcell®150	Heraeus, Hanau, Germany
Liquid nitrogen tank	L-240 K series	Taylor-Wharton, Camp Hill, PA, USA
Luminometer	Sirius Luminometer	Berthold Detection Systems, Pforzheim, Germany
Magnetic cell sorting (MACS)		Miltenyi Biotech, Bergisch Gladbach, Germany
Microbeads anti-PE		Miltenyi Biotech, Bergisch Gladbach, Germany
Microarray Chip	HumanGene 1.0 ST arrays	Affymetrix, Santa Clara, USA
Microarray Chip	GeneChip® HG- U133A	Affymetrix, Santa Clara, USA
Microliter syringe	710NR	Hamilton, Bonaduz, Switzerland
Micropipettes		Eppendorf, Hamburg, Germany

Microscope	AxioVert 100	Zeiss, Jena, Germany
Microscope		Leica, Wetzlar, Germany
Microwave oven		AEG, Nürnberg, Germany
Mini centrifuge	MCF-2360	LMS, Brigachtal, Germany
Multichannel pipette		Eppendorf, Hamburg, Germany
PCR cycler	iCycler	BioRad, Richmond, CA, USA
Pipetting assistant	Easypet®	Eppendorf, Hamburg, Germany
Power supplier	Standard Power Pack	Biometra, Göttingen, Germany
Real Time PCR	7300 Real-Time PCR	Applied Biosystems, Darmstadt, Germany
Shaker	Polymax 2040	Heidolph Instr., Schwabach, Germany
Spectrophotometer	Biowave II	Biochrom, Berlin, Germany
Sterile Bench		Heraeus, Hanau, Germany
Vortexer	Vortex-Genie 2	Scientific Industries, Bohemia, NY, USA

| Water Purification System | TKA GenePure | TKA, Niederelbert, Germany |

2.1.8 Softwares

Cellquest Pro software	BD Biosciences, Heidelberg, Germany
CpG plot software	European Bioinformatics Institute www.ebi.ac.uk/tools/emboss/cpgplot
Genesis	(Sturn et al., 2002)
GSEA tool	www.broad.mit.edu/gsea (Subramanian et al., 2005)
NIH Image J counting tool	www.rsbweb.nih.gov/ij
Oncomine™	www.oncomine.org
P-match program	www.gene-regulation.com
Uniprot protein knowledgebase	www.uniprot.org → UniprotKB → MLXIP
R2 microarray analysis and visualization platform	http://r2.amc.nl
Venn diagram generator software	www.pangloss.com/Seidel/protocols/venn.cgi

2.1.9 Antibodies

Antibody against	Fluorochrome	Manufacturer
CD10	PE	BD Biosciences, Heidelberg, Germany

CD10	PE	Leica Biosystems Newcastle Ltd, New Castle Upon Tyne, UK
CD20	APC	BD Biosciences, Heidelberg, Germany
CD22	FITC	BD Biosciences, Heidelberg, Germany
CD24	PE	BD Biosciences, Heidelberg, Germany
CD45 anti-human	PE	BD Biosciences, Heidelberg, Germany
CD45 anti-mouse	PE	BD Biosciences, Heidelberg, Germany
CD79a	APC	BD Biosciences, Heidelberg, Germany

2.1.10 siRNAs

AllStars negative control siRNA	#1027280	Qiagen, Hilden, Germany
Hs_MLXIP_1	Target sequence: 5'-CAGGACGATGA-CATGCTGTAT-3'	Qiagen, Hilden, Germany
Hs_MLXIP_3	Target sequence: 5'-CACAGTTTAGAT-CCAGTTGGA-3'	Qiagen, Hilden, Germany

2.1.11 Primer assays

All TaqMan® Gene Expression Assays were obtained from Applied Biosystems, Darmstadt, Germany or Metabion, Martinsried, Germany as indicated.

2.1.12 NOD-SCID mice

NOD-SCID mice were obtained from Charles River Laboratories, Calco, Italy. Mice were maintained in a TU München Division of Animal Resources facility under pathogen-free conditions in accordance with the institutional guidelines and approval of the local authorities (Regierung von Oberbayern, reference number 2531-42-10). Experiments were conducted according to the national animal welfare law (Tierschutzgesetz) and approved by the TU München Institutional Animal Care and Use Committee.

The NOD-SCID mice were monitored daily to identify any mice with burden of malignant disease. Mice were evaluated for any visible or palpable lumps, a hunched posture, tachypnea, a swollen belly, or ruffled fur and sacrificed promptly upon the appearance of any such symptoms.

2.2 Methods

2.2.1 Cell culture

Cells were grown in plastic cell culture flasks in a humidified incubator at 37°C in 5% CO_2 atmosphere in RPMI 1640 media (Invitrogen, Karlsruhe, Germany) containing 20% heat-inactivated fetal bovine serum (Biochrom, Berlin, Germany), 1% glutamine, 100 µg/mL gentamycin (Invitrogen) and 200 mg/dL D-glucose or 0 mg/dL D-glucose. All cell lines were checked routinely for purity and mycoplasma contamination using the commercial MycoAlert® Mycoplasma Detection Kit according to the manufacturer's manual. Only mycoplasma-free cell cultures were used for further analyses. All reagents were purchased from Sigma (Deisenhofen, Germany) if not otherwise specified.

Depending on the number of cells needed for analyses, cell lines were grown in middle-sized culture flasks (75 cm^2) containing 20 mL of medium or in large-sized culture flasks (175 cm^2) with 30 mL of medium. Saturated cultures were split 1:2 to 1:5 every 2–3 days and cells were resuspended in an appropriate volume of fresh medium. As leukemia cells grow in suspension, they could easily be removed from the flasks with the medium, centrifuged at 1,200 rpm for 7 min, resuspended, and spread in new culture flasks. Dislodged cells were then centrifuged as described above, resuspended, and disseminated in new culture flasks.

For long-term storage in liquid nitrogen (-192°C) cells were resuspended at a concentration of 1 x 10^6 to 1 x 10^7 per 1 mL FBS/10% DMSO, and 1 mL aliquots of the cell suspension were transferred into prepared cryovials. For controlled freezing the vials were put into freezing boxes containing

isopropanol and stored 12-24 hours at -80°C, before being moved into the liquid nitrogen freezer for further storage.

To re-culture the frozen cells, vials were removed from liquid nitrogen and thawed at room temperature until the cell suspension started to defrost. In order to remove toxic DMSO the cell suspension was transferred into a 50 mL Falcon tube carrying 5 mL of fresh standard medium, and cells were pelletized at 1,200 rpm for 7 min in a centrifuge. Subsequently the pellet was resuspended in fresh medium, and the suspension was transferred into a middle-sized culture flask and stored in an incubator.

For most analyses cell counts had to be determined by use of a Neubauer hemocytometer. Therefore 10 µL of Trypan Blue was added to a small volume of cell suspension (10-40 µL), and viable cells, which excluded the stain, were counted under a light microscope.

2.2.2 Preparation of ALL cells, PBMCs and FEB cells

ALL samples were obtained from bone marrow aspirates (n = 24) or peripheral blood (n = 1) of children with ALL prior to therapy obtained from the Departments of Pediatrics of the Universities of Halle-Wittenberg and Leipzig as well as the ALL-BFM study group of the Society of Pediatric Oncology and Hematology (GPOH). Flow cytometric assessment of CD10 and CD19 confirmed the presence of leukemic blasts (> 90% of cells) in each ALL sample. PBMCs were isolated by centrifugation over Ficoll-Paque (GE Healthcare, Freiburg, Germany) from adult healthy donors. FEB highly expressing the early B cell markers CD10 and CD19 were isolated from umbilical cord blood samples. CD19$^+$ cells were purified with CD19

Dynabeads (Dynal Biotech, Oslo, Norway) and magnetic cell sorting (MACS, Miltenyi Biotech, Bergisch Gladbach, Germany). Dynabeads were removed with DETACHaBEAD CD19 (Invitrogen). After detachment CD19$^+$ cells were stained with anti-CD10-PE antibody (BD Biosciences, San Jose, CA) and subsequently with anti-PE microbeads and purified via MACS (both Miltenyi Biotech).

2.2.3 RNA extraction and quantitative real-time PCR (qRT-PCR)

RNA was isolated using the RNeasy RNA isolation kit (Qiagen, Düsseldorf, Germany) according to the manufacturer´s instructions. Gene expression was analyzed by qRT-PCR using TaqMan Universal PCR Master Mix (Applied Biosystems, Darmstadt, Germany) and fluorescence detection with an AB 7300 Real-Time PCR System (Applied Biosystems). Gene specific primers and probes were obtained as TaqMan Gene Expression Assays (Applied Biosystems), which consisted of a FAM dye-labeled TaqMan MGB probe and two unlabeled PCR primers; 20x stock solutions of these reagents were added to the TaqMan Universal PCR Master Mix with cDNA at a volume of 25 µL. Results were normalized to the established leukemia housekeeping gene *beta-2-microglobulin (B2M)* (Subramanian et al., 2005) and quantified by the ddCt-method. The concentration of primers and probes were 900 and 250 nM, respectively. Inventoried TaqMan® Gene Expression Assays (Applied Biosystems) were used for *B2M* (Hs00187842_m1), *ABL1* (Hs01104721_m1), *MondoA* (Hs00208850_m1), *MondoB* inventoried (inv) (Hs00263027_m1), *MondoB* made-to-order (mto) (Hs00975714_m1), *MLX* (Hs00273744_m1), *RUNX1* (Hs01021967_m1), *TGFBR2* (Hs00234235_m1), *DNTT*

(Hs00172743_m1), *PDGFRA* (Hs00998026_m1), and *DDIT3* (Hs01090850_m1).

2.2.4 MondoA isoforms

Analysis of MondoA isoforms was performed with uniprot protein knowledgebase (www.uniprot.org → UniprotKB → MLXIP). The inventoried TaqMan® Gene Expression Assay (Hs00208850_m1, Applied Biosystems) detects *isoforms 1 and 3* (exon 9-10, sequence PPAQIESILP). A made-to-order TaqMan® Gene Expression Assay (Applied Biosystems) was used for *MondoA* isoforms *1, 2 and 4* (Hs00917077_m1, exon 12-13, sequence VTGPSIRDCPN), another made-to-order TaqMan® Gene Expression Assay (Metabion, Martinsried, Germany) was used for *MondoA isoforms 3 and 5* (MondoA sense oligo sequence: 5´-AACTTTTGTGCACCCCAAAC-3´, MondoA antisense oligo sequence: 5´-GGATGGGAAAACATCCCTCT-3', exon 10, sequence NARIAPIGEPGGET).

2.2.5 Promoter analysis

Prediction of putative conserved transcription factor binding sites was performed with the P-match™ program (available at www.gene-regulation.com) (Chekmenev et al., 2005) analyzing the first 10,000 base pairs upstream of the predicted transcriptional start site (TSS) of the *MondoA* gene. Prediction and analysis of CpG-islands was performed with the CpG plot software of the European Bioinformatics Institute (available at www.ebi.ac.uk/Tools/emboss/cpgplot).

2.2.6 Inhibition of DNA methylation

Nalm6 and cALL2 cells were incubated for 72h in RPMI 1640 media containing 200 mg/dL D-glucose (Invitrogen) supplemented with 50 to 75 mM dimethyl sulfoxide (DMSO) or 50 mM and 75 mM zebularine (Sigma; dissolved in DMSO), respectively. Media and DMSO or zebularine were renewed every 24h. After 72h cells were harvested and RNA was extracted as described above.

2.2.7 Constructs, retroviral gene transfer and RNA interference (RNAi)

For stable silencing of MondoA expression, oligonucleotides of the short hairpin (sh) corresponding to a MondoA small interfering RNA (siRNA) were cloned into the retroviral pSIREN-RetroQ vector (Takara Bio Europe/Clontech). Retroviral constructs were transfected by electroporation into PT67 packaging cells, and viral supernatant isolated 48h after transfection. Infection of target cells (Nalm6) was carried out in the presence of 4 µg/mL polybrene. Single cell cloned stable infectants were isolated after selection in 2 µg/mL puromycin (pSIREN-RetroQ) for at least seven days and were first used for subsequent assays after at least 7 additional days in culture without puromycin to avoid biases through acute infection and/or puromycin toxicity. The siRNA target sequences of Hs_MLXIP_1 (SI04144469) and Hs_MLXIP_3 (SI04371052) (Qiagen GmbH, Hilden, Germany) were 5'-CAGGACGATGACATGCTGTAT-3' and 5'-CACAGTTTAGATCCAGTTGGA-3', respectively. As a control the corresponding shRNA of the AllStars negative control siRNA (#1027280, Qiagen) was used. Each experiment shown in this study analyzing stably

MondoA silenced Nalm6 cells (referred to as "pSImondoA" cells) compared to non-silenced Nalm6 cells (referred to as "pSInegative" cells) was performed with at least three independent infectants expressing either shMLXIP_1 or shMLXIP_3.

2.2.8 Microarray analysis

Microarray analyses were performed at the University of Halle (HG-U133A arrays, experimentators: Prof. Dr. Martin Staege and Dr. Uwe Hattenhorst) and in the Expression Core Facility of the TU München (Affymetrix Human Gene 1.0 ST arrays, experimentator: Olivia Prazeres da Costa, M.Sc.). Total RNA was amplified and labeled using Affymetrix GeneChip Whole Transcript Sense Target Labeling Kit according to the manufacturer's protocol. cRNA was hybridized to Affymetrix Human Gene 1.0 ST arrays or HG-U133A arrays. Arrays were either RMA-normalized (Human Gene 1.0 ST) or scaled to the same target intensity of 500 (default setting) using trimmed mean signal of all probe sets (HG-U133A). Quality assessment consisted of RNA degradation plots, Affymetrix control metrics, sample cross-correlation, and probe-level visualizations. RMA-normalization incorporated (separately for each RNA type data set) background correction, quantile normalization, and probe-level summation. Microarray data were deposited at the Gene Expression Omnibus (GSE34670 and GSE33967). Subsequent data analysis was carried out with signal intensities that were log2 transformed for equal representation of over- and under-expressed genes and then median centered to remove biases based on single expression values. Unsupervised hierarchical clustering (Eisen et al., 1998) and principal component analysis were accomplished by

use of Genesis software package (Sturn et al., 2002). For identification of differentially expressed genes we used significance analysis of microarrays (SAM) (Tusher et al., 2001). Gene-set enrichment analysis (GSEA) and pathway analyses were performed with the GSEA tool (available at www.broad.mit.edu/gsea) (Subramanian et al., 2005). Comparison of independent published microarray studies was performed with the R2 microarray analysis and visualization platform (http://r2.amc.nl). All published datasets analyzed with the R2 platform were generated with Affymetrix HG-U133 Plus 2.0 GeneChips and expression data were normalized with the MAS5.0 algorithm within the Affymetrix GCOS program. Genes-in-overlap analysis was performed with the Venn diagram generator software (available at www.pangloss.com/seidel/protocols/venn.cgi).

2.2.9 Metabolomics

In cooperation with the Helmholtz Center Munich (experimentators: Prof. Dr. Jerzy Adamski, Dr. Cornelia Prehn, Dr. Julia Scarpa), a metabolomic analysis of two pSInegative and three pSImondoA clones was performed with the Absolute IDQ-Kit (Biocrates Life Sciences AG, Innsbruck, Austria) according to the manufacturers protocol. $2,5 \times 10^6$ cells/clone as a pellet were choc frozen in nitrogen and stored at - 80°C. 163 intracellular metabolites (amino acids, hexoses, carnitines, sphingomyelines, glycerophospholipids) were analyzed.

2.2.10 Metabolism assays

Media turnover and metabolic activity of leukemia cells was assessed as follows: 3×10^6 pSInegative and pSImondoA Nalm6 infectants were incubated for 72h in 20 mL RPMI 1640 media containing 200 mg/dL D-glucose and phenol red. Thereafter, the production of lactic acid was measured in cell-free conditioned media by photometrical determination (IMPLEN GmbH, Munich, Germany) of oxidized phenol red at its absorption maximum of 557 nm in phosphate containing buffers (Howard W. Robinson and Corinne G. Hogden, 1941) (such as RPMI 1640 media).

2.2.11 Analysis of glucose concentrations

Glucose levels of conditioned media were analyzed with a commercial Breeze 2 glucometer (Bayer Vital GmbH, Leverkusen, Germany) in an aliquot (5 µL) of cell-free conditioned media according to the manufacturer's protocol. Each measurement was performed in duplicate.

2.2.12 Bromodeoxyuridine (BrdU) proliferation assay

2×10^4 cells/well (octaplicates/group) on a 96-well-plate were incubated for 48h in 200 µL RPMI 1640 media containing 200 mg/dL D-glucose. Then cells were incubated with the 5-bromo-2′-deoxyuridine (BrdU)-labeling solution (Roche, Basel, Switzerland) for 14h. Fixation, detection and colorimetric reaction were performed according to the manufacturer's protocol. Absorption was measured with a Multiscan Ascent plate reader (Thermo Fisher Scientific, Dreieich, Germany).

2.2.13 Flow cytometry

Cells were harvested, prepared and stained using propidium iodide (Sigma) for cell cycle analysis as previously described (Grunewald et al., 2012). The annexin-V-PE/7-AAD (7-aminoactinomycin-D) apoptosis detection kit 1 (Beckton Dickinson) was used to assess apoptosis and necrosis. Cluster of differentiation (CD) molecules were analyzed using antibodies (all Becton Dickinson) against CD20 (fluorochrome: APC, Lot: 53339), CD22 (fluorochrome: FITC, Lot: 30141), CD24 (fluorochrome: PE, Lot: 23219) and CD79a (fluorochrome: APC, Lot: 91346). Samples were analyzed on a FACScalibur flow cytometer using Cellquest Pro software (both Becton Dickinson). At least 30,000 events/sample were recorded.

2.2.14 Assessment of clonogenicity

Clonogenicity of leukemia cells was assessed with a commercial colony-forming assay (R&D Systems, Wiesbaden-Nordenstadt, Germany). Leukemia cells were seeded at a density of $5x10^3$ cells per 1.5 mL methylcellulose-based media into a 35-mm plate and cultured for 14 days at 37°C and 5% CO_2 in a humidified atmosphere. Number of colonies was counted with the NIH Image J counting tool.

2.2.15 MondoA NOD-SCID mouse model

13 unconditioned non - obese diabetic - severe combined immunodeficiency (NOD-SCID) mice were transplanted by intravenous injection of $2x10^6$ cells into the tail vein, five mice with Nalm6 pSInegative cells and eight mice with two different Nalm6 pSImondoA cells. Two of the eight pSImondoA mice died

during observation, probably due to infection, as they did not show any sign of leukemic burden in necropsy. Mice were weighed at the start, after two weeks and after five weeks of the experiment to observe any weight loss as a sign of illness. After five weeks, all mice were sacrificed on the same day and liver, spleen, and central and peripheral lymph nodes were prepared, weighed and sent to pathology for histology and immunohistochemistry to detect leukemic infiltrates. Furthermore, peripheral blood smears were performed and stained with an antibody against CD10 (Beckton Dickinson) as a common marker on the surface of ALL cells. Finally, peripheral blood and bone marrow samples were stained with human and murine antibodies against CD45 (Beckton Dicksinson) for flow cytometry to determine the fraction of human CD45 as a sign for leukemic blasts.

2.2.16 Histology and immunohistochemistry

Organs of 11 NOD-SCID mice were fixed in 4 % formaldehyde and embedded in paraffin. Three to five µm thick sections from all tissues were cut and stained with hematoxylin and eosin (H&E). All sections were reviewed by two pathologists (Dr. med. Melissa Schlitter and Prof. Dr. med. Irene Esposito, both Institute of Pathology, Klinikum rechts der Isar, TU München).

Immunohistochemistry was performed using an automated immunostainer with an iVIEW DAB detection kit (Ventana Medical System, Roche, Mannheim, Germany) according to the company's protocols for open procedures with slight modifications. The following antibody was used: mouse monoclonal anti-CD10 (dilution 1:10, NCL-L-CD10-270, Clon 56C6, Leica Biosystems Newcastle Ltd, New Castle Upon Tyne, UK). For antigen retrieval,

boiling in EDTA buffer (pH 9) for 60 min was performed prior to CD10 staining.

2.2.17 Statistical analysis

Data were analyzed by unpaired two-tailed student's t-test, two-tailed Fisher's exact test or Spearman correlation test as indicated. P values < 0.05 were considered significant.

3 Results

3.1 MondoA is highly and stably overexpressed in leukemia

The previous microarray analysis of 25 primary early pre-B cell ALL samples versus 9 highly purified fetal early pre-B cell samples (FEB; fraction of CD10$^+$ and CD19$^+$ cells of >82%) (GSE34670) by Richter et al. (Richter et al., 2005) revealed that MondoA is highly overexpressed in leukemia. This observation was extended by matching these microarray data against a published study of 36 normal adult and fetal tissues (GSE2361) (Ge et al., 2005), which demonstrated that MondoA is only expressed at very low levels in FEB and in normal tissues compared to early pre-B cell ALL samples (**Figure 5A**).

To further confirm the high MondoA overexpression in ALL, the author of this dissertation performed an expression analysis of 21 different T cell and B cell lineage ALL lines that exhibited a high MondoA overexpression (defined as expression higher than in FEB) in 12 cell lines (57.1%) (**Figure 5B**).

These data were further validated using the R2 microarray analysis and visualization tool (http://r2:aml.nl) by comparison of a pre-B cell ALL study with that of an acute myeloid leukemia (AML), a whole blood and two independent normal tissue studies (**Figure 5C**) (Rhodes et al., 2004; Roth et al., 2006; Balgobind et al., 2011).

Additionally, MondoA overexpression in ALL was confirmed by reanalysis of two independent published microarray studies that directly compared B cell lineage ALL samples with peripheral blood mononuclear cells (PBMCs) or bone marrow (BM) (**Figure 5D**) (Andersson et al., 2007; Haferlach et al., 2010).

As B cell lineage ALL comprises the most common type of leukemia among children (Pui et al., 2011), four B cell lineage ALL lines were chosen for further investigation - two with high (Nalm6, RS4;11) and two with low MondoA expression (SD-1, cALL2). As seen in **Figure 5E**, MondoA proved to be expressed in a remarkably stably fashion, almost without any oscillation (note small error bars).

Interestingly, the binding partner of MondoA, MLX, is strongly coexpressed with MondoA ($r_{Spearman}$ = 0.77, 95%CI: 0.5 to 0.9, p < 0.0001, n = 21 cell lines) (**Figure 5F**).

However, the MondoA paralog and additional MLX binding partner MondoB (Iizuka et al., 2004; Ishii et al., 2004), is neither expressed in the MondoA-high nor MondoA-low ALL lines (tested with two different MondoB primer assays and increasing cDNA employment), whereas the transcript could be readily detected in the human hepatocellular carcinoma lines HepG2 and Hep3B (positive controls) (**Figure 5G**).

Taken together, these data provide evidence that MondoA, but not MondoB, is highly and stably overexpressed in human ALL compared to normal adult tissues including FEB, BM and PBMCs.
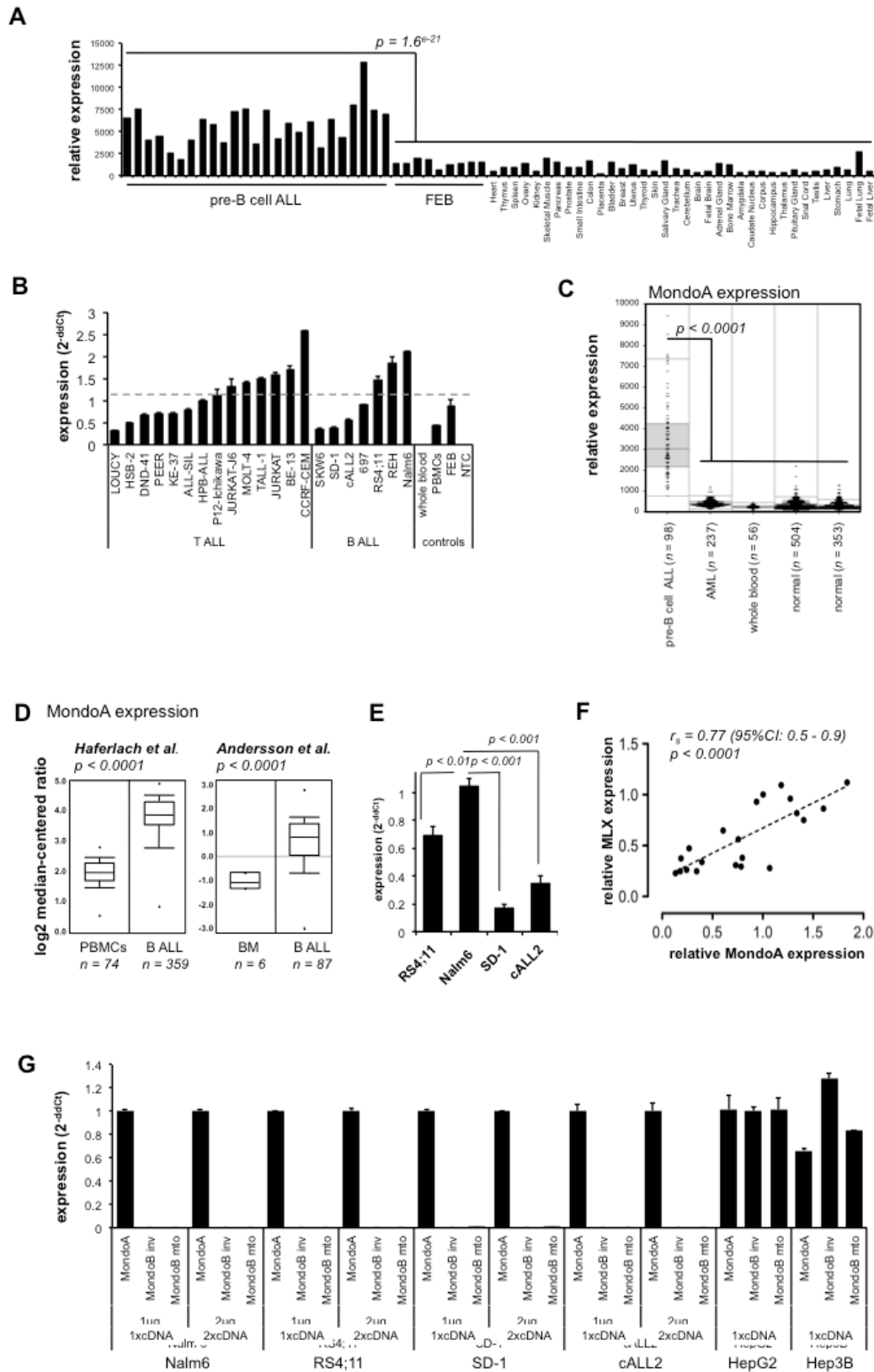
Figure 5 - MondoA is highly and stably overexpressed in leukemia

(A) Relative expression of MondoA in 25 primary childhood early pre-B cell ALL, 9 FEB samples and 34 normal adult tissues as assessed by microarrays (GSE34670 and GSE2361). T-test.

(B) Expression analysis of 14 cultured T cell and 7 B cell lineage ALL lines for MondoA by qRT-PCR. RNA from whole blood, PBMCs and FEB of healthy donors were used as controls. NTC = no template control. Data are mean ± SEM. HPB-ALL was set as one. The dashed line is adjusted to the mean MondoA expression of FEB.

(C) Box-dot-plots showing MondoA expression in pre-B cell ALL (GSE7440), AML (GSE17855), whole blood (GSE6575), and normal tissues (GSE7307; GSE3526).

(D) Analysis of MondoA expression in two published independent microarray datasets (GSE13204 (Haferlach et al., 2010); GSE7186 (Andersson et al., 2007)) in primary B ALL and bone marrow (BM) or PBMCs. Data were retrieved via the oncomine™ cancer versus normal tissue search tool (available at www.oncomine.org (Rhodes et al., 2004)). Box-plots indicate the median expression and 25th and 75th percentile, respectively. Whiskers indicate the 10th and 90th percentile. Outliers are displayed as black dots.

(E) Summary of multiple ($n \geq 10$ per cell line) expression analyses of human B ALL cell lines RS4;11, Nalm6, SD-1 and cALL2 by qRT-PCR. Please note the remarkably stable MondoA expression indicated by very small error bars. Data are mean ± SEM.

(F) Correlation analysis of MondoA and MLX by qRT-PCR of the 21 ALL cell lines seen in (B) by qRT-PCR. Each dot represents the mean expression value(s) of two independent experiments. Expression of MLX and MondoA in HPB-ALL were set as one. The dashed line indicates the computed linear regression. Spearman test.

(G) Expression analysis of MondoA and MondoB in Nalm6 and RS4;11 cells by qRT-PCR. For positive controls the hepatocellular carcinoma lines HepG2 and Hep3B were used. For MondoB detection two different TaqMan Gene Expression Assays were used (MondoB inv and MondoB mto). The qRT-PCR analyses were performed with standard amount of cDNA (1 x cDNA) and doubled amount of cDNA (2 x cDNA). Data are mean ± SEM of two independent experiments (duplicates/group); t-test.

3.2 MondoA has five isoforms

As two different MondoA Western Blot antibodies detected bands at 69 kDa and 39 kDa rather than at 101 kDa as the molecular weight of MondoA, we performed an in-silico analysis within the uniprot knowledgebase that revealed five MondoA isoforms by alternative splicing. Nevertheless, as shown in **Table 1**, only isoform 1 presents all necessary functional domains. The mitochondrial targeting sequence is necessary for localization at the outer mitochondrial membrane. The Mondo conserved region (MCR) is required for cytoplasmatic localization. The transcription activation domain (TAD) is necessary for activation, whereas the DNA - binding domain enables nuclear

DNA - binding. Finally, the bHLHZip domain is crucial for the affiliation to the Mondo family and the MLX - dimerization domain permits shuttling to the nucleus. Expression analysis with primer assays targeting the different isoforms showed that possibly all isoforms are expressed, with highest expressions of isoforms 1 and 3. The Applied Biosystems inventoried TaqMan gene expression assay used in this work only targets isoforms 1 and 3.

Since important functional domains such as the DNA binding and the MLX dimerization domain are missing in isoform 3, isoform 1 was concluded to be responsible for the MondoA effects observed in this work.

Figure 3 – functional structure of MondoA
(MCR) MondoA conserved region, (TAD) Transcriptional activation domain, (bHLHZip) basic helix-loop-helix leucine zipper, (MlxH) dimerization with MLX cytoplasmic retention domain

Isoform	Mitochondrial targeting sequence	Mondo conserved region	Trans-activation domain	DNA binding domain	bHLHZip domain	MLXIP/MLX dimerization domain
1	x	X	x	x	x	x
2			(x)	x	x	x
3	x	X	x			
4			(x)	x	(x)	
5			(x)			

Table 1 – MondoA has five isoforms
Analysis of MondoA isoforms was performed with uniprot protein knowledgebase (www.uniprot.org → UniprotKB → MLXIP). The inventoried TaqMan® Gene Expression Assay (Hs00208850_m1, Applied Biosystems) detects *isoforms 1 and 3* (exon 9-10, sequence PPAQIESILP). A made-to-order TaqMan® Gene Expression Assay (Applied Biosystems) was used for *MondoA* isoforms *1, 2 and 4* (Hs00917077_m1, exon 12-13, amino acid sequence VTGPSIRDCPN), another made-to-order TaqMan® Gene Expression Assay (Metabion, Martinsried, Germany) was used for *MondoA isoforms 3 and 5* (MondoA sense oligo sequence: 5´- AAC TTT TGT GCA CCC CAA AC – 3´, MondoA antisense oligo sequence: 5´- GGA TGG GAA AAC ATC CCT CT – 3, exon 10, amino acid sequence NARIAPIGEPGGET).

X expressed, (X) only partially expressed

3.3 MondoA expression can be modulated by lactate and DNA methylation and correlates with RUNX1 expression

Glucose and lactate have been previously reported to be potent stimuli for MondoA in breast cancer cells and murine embryonic fibroblasts (MEFs) (Chen et al., 2010; Peterson et al., 2010). To determine whether MondoA is regulated by these metabolites in leukemia, the author of this dissertation performed expression analyses after incubation of RS4;11 and Nalm6 lines for 24h and 48h in media without glucose or media supplemented with 200 mg/dL D-glucose and with or without addition of 15 mmol/L lactate. These experiments showed no significant impact of glucose deprivation on MondoA expression, but a significant suppression of MondoA expression by lactate (**Figure 6A**).

To find potential transcription factors that might drive MondoA expression, the author of this dissertation next performed an *in silico* promoter analysis that predicted two conserved CpG-islands, which are flanked by six conserved binding sites for the runt-related transcription factor 1 (RUNX1, also known as AML1) that is the top-ranked transcription factor as it occupies six out of 13 predicted transcription factor binding sites (**Figure 6B** and **Table 2**). Of note,

similar to the strong correlation of MondoA and MLX expression, the author also found a striking correlation between MondoA and RUNX1 expression in T cell and B cell lineage ALL lines ($r_{Spearman}$ = 0.74, 95%CI: 0.44 to 0.89; $p <$ 0.0001, n = 21 cell lines) (**Figure 6C**).

In support of the premise that MondoA may be transcriptionally regulated via DNA methylation, the DNA methylation blocker zebularine was found to increase MondoA expression in leukemia cells (**Figure 6D**), whereas the well-known leukemia housekeeping gene *Abelson tyrosine-protein kinase 1* (*ABL1*) (Beillard et al., 2003) was not regulated by zebularine treatment (**Figure 6D**).
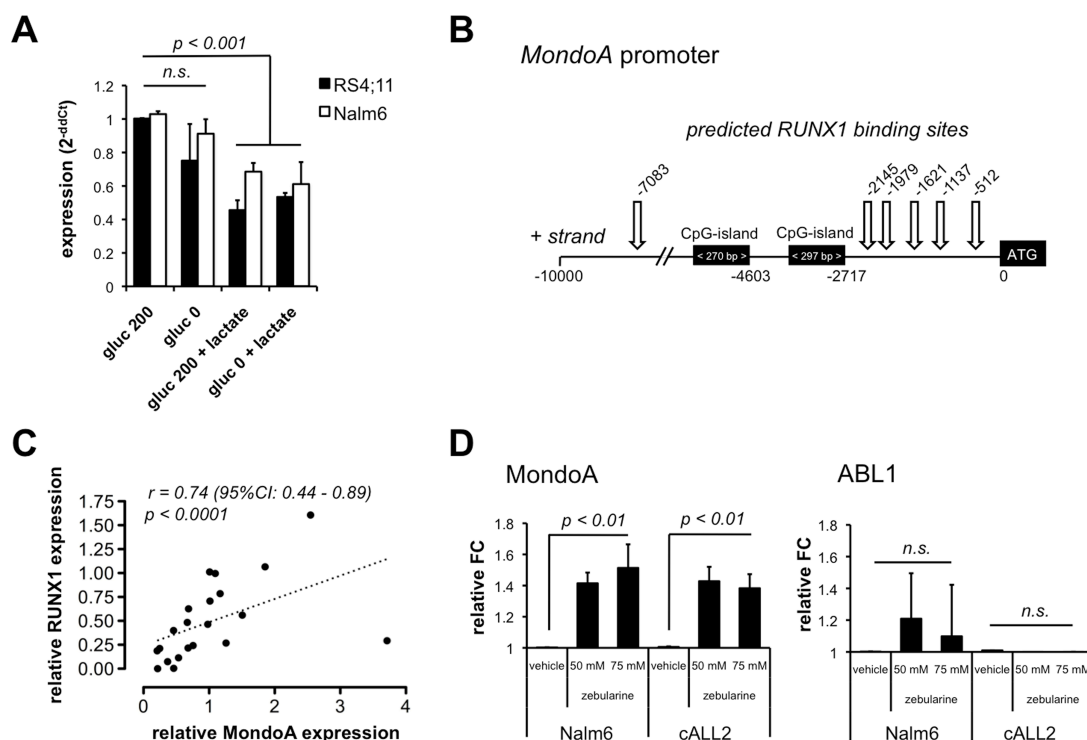

Figure 6 – MondoA expression can be modulated by lactate and DNA methylation and correlates with RUNX1 expression
(A) Analysis of MondoA expression by qRT-PCR of human B cell lineage ALL RS4;11 and Nalm6 lines. 4×10^6 cells were incubated for 24h in 20 mL RPMI 1640 media supplemented with 200 mg/dL or 0 mg/dL D-glucose and with or without

addition of 15 mmol/L lactate. Data are mean ± SEM of three independent experiments (duplicates/group); t-test.

(B) Schematic illustration of the results of the *in silico* promoter analysis of the *MondoA* promoter. The CpG-islands including their corresponding length in base pairs (bp) are displayed as black boxes. White arrows point on predicted RUNX1 binding sites.

(C) Correlation analysis of MondoA and RUNX1 by qRT-PCR of 21 ALL cell lines seen in Figure 5B by qRT-PCR. Each dot represents the mean expression value of two independent experiments. RUNX1 and MondoA expression in HPB-ALL were set as one. The dashed line indicates the computed linear regression. Spearman test.

(D) Analysis of MondoA and ABL1 expression in Nalm6 and cALL2 cells preincubated for 24h with 50 mM and 75 mM of the demethylation reagent zebularine or vehicle (DMSO). Data are mean ± SEM of three independent experiments (duplicates/group); t-test. FC = fold change.

Identifier	TF name	bp from TSS	Binding sequence (+ strand)	core match	matrix match
V$AP1_Q4	AP-1	-9036	agTGACTtagc	1	0.99
V$LYF1_01	LYF-1	-8565	ttTGGGAgg	1	0.99
V$LYF1_01	LYF-1	-8246	ttTGGGAgg	1	0.99
V$AML1_01	RUNX1	-7083	tGTGGT	1	1
V$NFAT_Q6	NF-AT	-5254	tcatGGAAAatt	1	0.99
V$LYF1_01	LYF-1	-2246	ttTGGGAgg	1	0.99
V$AML1_01	RUNX1	-2145	tGTGGT	1	1
V$AML1_01	RUNX1	-1979	tGTGGT	1	1
V$AML1_01	RUNX1	-1621	tGTGGT	1	1
V$AML1_01	RUNX1	-1137	tGTGGT	1	1
V$NFAT_Q6	NF-AT	-1006	acttGGAAAact	1	0.98
V$AML1_01	RUNX1	-512	tGTGGT	1	1
V$NFAT_Q6	NF-AT	-476	ttatGGAAAatt	1	0.99

Table 2. List of predicted transcription factor (TF) binding sites within the human *MondoA* promoter. Promoter analysis was performed with the P-Match™ program (www.gene-regulation.com) interrogating the first 10,000 bp (plus strand) upstream of the predicted transcriptional start site (TSS). Only binding sites with minimum values of 0.98 in the core match and matrix match scores are listed.

3.4 MondoA expression increases metabolic activity

To test the functional role of MondoA in leukemia cells, knockdown experiments were performed. For this purpose, the author of this dissertation generated single cell-cloned MondoA-silencing or non-silencing shRNA expressing cell lines of the highly MondoA expressing parental B cell lineage ALL Nalm6 line [pSImondoA (either expressing shMLXIP_1 or shMLXIP_3, see methods section) and pSInegative, respectively] (**Figure 7A**). As a screening experiment for changes in the intracellular metabolism, a metabolomic analysis with mass spectrometry of two pSInegative against three pSImondoA clones was performed in cooperation with the Helmholtz Center Munich (experimentators: Prof. Dr. Jerzy Adamski, Dr. Cornelia Prehn, Dr. Julia Scarpa), which evidenced a downregulation of intracellular glucose to 61% in the pSImondoA clones. Besides, intracellular serines were 125% upregulated and intracellular sphingolipids downregulated to 80% (**see Supplementary Table 4**).

The author then investigated the impact of different MondoA expression levels on the metabolic activity and glucose utilization. To this end, MondoA-suppressed Nalm6 clones and respective controls were incubated in RPMI 1640 media containing 200 mg/dL D-glucose for 72h and media turnover and media glucose levels were measured thereafter. As expected, constitutive MondoA knockdown proved to reduce the metabolic activity of leukemia cells, which led to a higher amount of remaining non-metabolized glucose in the conditioned culture media (**Figure 7B-C**).
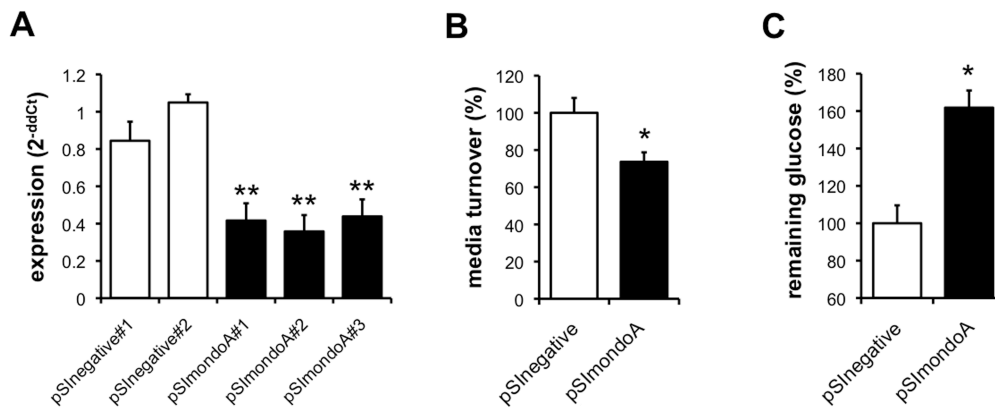
Figure 7 – MondoA expression increases metabolic activity
(A) MondoA expression in Nalm6 cells either expressing nonsense shRNA (clones #1 and #2, hereafter summarized as pSInegative) or specific MondoA shRNAs (clone #1 = shMLXIP_1 and clones #2 and #3 = shMLXIP_3; hereafter summarized as pSImondoA). Mean±SEM of at least four independent measurements.
(B) Analysis of metabolic activity of pSInegative and pSImondoA Nalm6 cells. 3×10^6 cells/flask were incubated for 72h in 20 mL RPMI 1640 media containing 200 mg/dL D-glucose. Thereafter media turnover was quantified by photometry and normalized to cell count. Data are mean ± SEM of three independent experiments (duplicates/group); t-test.
(C) Analysis of remaining media D-glucose after 72h. Data are mean ± SEM of three independent experiments (duplicates/group); t-test. *$p < 0.05$, **$p < 0.01$; t-test.

3.5 MondoA and TXNIP

Thioredoxin interacting protein (TXNIP) has been described as a direct transcriptional target of MondoA by Stoltzman CA et al. (Stoltzman et al., 2008, 2011). Originally characterized as an endogenous inhibitor of thioredoxin, a key regulator in cellular redox homeostasis, TXNIP is also known to play important roles in tumor growth and metastasis and glucose metabolism (Kim et al., 2007; Muoio, 2007; Parikh et al., 2007). These functions suggest a tumor suppressor function for TXNIP (Han et al., 2003).

Since interactions between MondoA and TXNIP in regulating glucose metabolism have been discussed in the literature (Chen et al., 2010;

Stoltzman et al., 2011), the author of this dissertation examined a correlation between MondoA and TXNIP expression in leukemia.

TXNIP expression was found to rise significantly in presence of abundant glucose (**Figure 8A-B**). Lactate has been described as a potent inductor of TXNIP expression in breast cancer cells (Chen et al., 2010), what the author could confirm in leukemia (**Figure 8B**). Interestingly, MondoA knockdown seemed to downregulate TXNIP expression (**Figure 8C**). On the other hand, the B ALL cells with high MondoA expression Nalm6 and RS4;11 tended to have lower TXNIP expression levels than the B ALL cells with low MondoA expression SD-1 and cALL2. Therefore TXNIP expression seems to be directly glucose dependent but not clearly correlated to MondoA expression in leukemia cells.
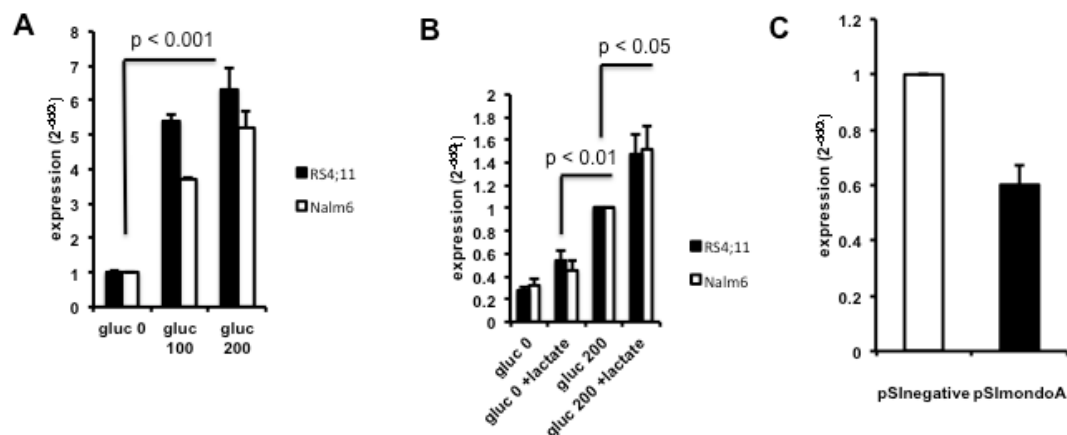
Figure 8 – TXNIP is induced by glucose and lactate
(A) Analysis of TXNIP expression by qRT-PCR of human B cell lineage ALL RS4;11 and Nalm6 lines. 4×10^6 cells were incubated for 24h in 20 mL RPMI 1640 media supplemented with 0 mg/dL, 100 mg/dL or 200 mg/dL D-glucose. Data are mean ± SEM of three independent experiments (duplicates/group); t-test.
(B) Analysis of TXNIP expression by qRT-PCR of human B cell lineage ALL RS4;11 and Nalm6 lines. 4×10^6 cells were incubated for 24h in 20 mL RPMI 1640 media supplemented with 0 mg/dL or 200 mg/dL D-glucose and with or without addition of 15 mmol/l lactate. Data are mean ± SEM of three independent experiments (duplicates/group); t-test.
(C) Expression analysis of TXNIP in Nalm6 cells expressing either a nonsense shRNA (pSInegative) or a MondoA shRNA (pSImondoA).

3.6 MondoA knockdown promotes differentiation

of leukemia cells

Microarray-based gene expression profiling has been used to identify prognosis- associated signatures in childhood ALL (Ferrando and Look, 2003; Ross et al., 2003; Willenbrock et al., 2004; Cario et al., 2005). To gain more functional insight in the effect of MondoA on leukemia, two different pSInegative Nalm6 clones and three different pSImondoA Nalm6 clones were subjected to a whole-transcriptome microarray analysis. MondoA knockdown differentially regulates 191 genes (mean log2 fold change ±0.5, $p < 0.05$, t-test) of which 49 genes were up- and 142 genes were downregulated (**Supplementary Table 1** and **Figure 9A**). Surprisingly, gene-set enrichment analysis (GSEA) did not only reveal strong enrichments of gene-sets involved in cellular metabolism, but most significantly enrichments of gene-sets involved in the maintenance of stemness, B cell differentiation as well as chemo/stress-resistance and survival (**Figure 9B** and **Table 3**). For instance, the gene-set STEMCELL_COMMON_DN (now renamed in RAMALHO_STEMNESS_DN) contains genes, which are usually depleted in embryonic, neural and hematopoietic stem cells (Ramalho-Santos et al., 2002), whereas the gene-set BLEO_HUMAN_LYMPH_HIGH_4HRS_UP comprises genes involved in DNA repair, cell cycle regulation, and apoptosis, which are differentially regulated in human lymphocytes 4h following treatment with a high dose of bleomycin (Islaih et al., 2004). To validate these microarray data, the author of this dissertation selected three up- and three downregulated genes of the 40 top-ranked genes according to their log2 fold change (**Figure 9A**), all of which have been previously associated with B cell

lineage ALL and B cell differentiation (Maytin and Habener, 1998; Coutts et al., 1999; Yeoh et al., 2002; Pereira et al., 2004; Massagué, 2008; Vladareanu et al., 2010; Karim et al., 2011). Their differential regulation upon MondoA knockdown was entirely confirmed on RNA or protein level by qRT-PCR or flow cytometry, respectively (**Figure 9C-D**). Moreover, apart from these differentiation markers, whose differential regulation seemed to take place on the transcriptional level (microarrays), the author also tested for the well-known B cell differentiation markers CD20 and CD24 (Fang et al., 2010; Raponi et al., 2011), which were not significantly regulated on RNA level. Strikingly, these molecules were significantly upregulated on the protein level in MondoA suppressed Nalm6 cells.

Taken together, these data suggest that MondoA knockdown results in a more differentiated phenotype of leukemia cells indicated by the transcriptional and post-transcriptional regulation of differentiation markers (**Figure 9C-D**).
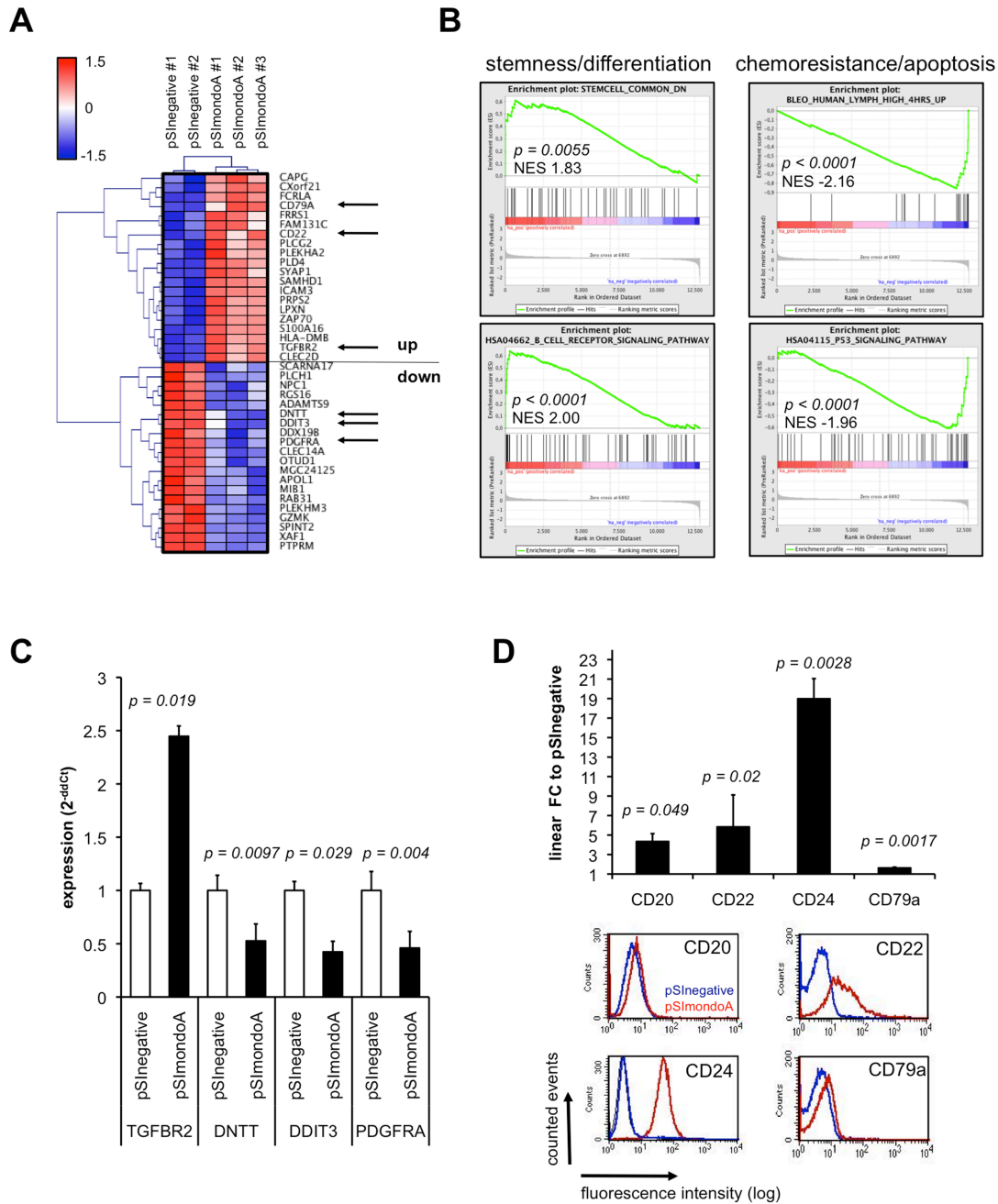
Figure 9 – MondoA knockdown promotes differentiation of leukemia cells
(A) Heatmap and hierarchical clustering of the top 40 up- and downregulated genes (log2 transformed values) after MondoA knockdown as identified by DNA microarrays (GSE33967, Affymetrix Human Gene 1.0 ST arrays). Nalm6 pSImondoA#1 expresses shMLXIP_1, Nalm6 pSImondoA#2 and #3 express shMLXIP_3 (see methods section). Arrows mark genes selected for validation by qRT-PCR or flow cytometry.
(B) Enrichment plots of significantly enriched gene-sets identified by gene-set enrichment analysis (GSEA). NES = normalized enrichment score.
(C) Gene expression analysis of differentially regulated genes by qRT-PCR. TGFBR2: transforming growth factor beta receptor 2, DNTT: terminal deoxynucleotidyl-transferase, PDGFRA: platelet-derived growth factor receptor alpha,

DDIT3: DNA-damage-inducible transcript 3. Data are mean ± SEM of two independent experiments (duplicates/group); t-test.
(D) Expression analysis of the surface molecules CD20, CD22, CD24 and CD79a in pSInegative and pSImondoA Nalm6 cells by flow cytometry. Bar graphs show the linear fold changes of pSImondoA/pSInegative. Data are mean ± SEM of two independent experiments (at least duplicates/group); t-test. Flow cytometry images show representative measurements for the indicated cell surface marker.

Gene-set name	NES	Nominal p-value	Involvement in
HSA04662_B_CELL_RECEPTOR_SIGNALING_PATHWAY	2.00	< 0.0001	Differentiation
MENSSEN_MYC_UP	1.84	0.0056	Proliferation
STEMCELL_COMMON_DN	1.83	0.0055	Stemness
HSA04612_ANTIGEN_PROCESSING_AND_PRESENTATION	1.83	< 0.0001	Differentiation
SCHUMACHER_MYC_UP	1.83	< 0.0001	Proliferation
HSA00230_PURINE_METABOLISM	1.81	< 0.0001	Metabolism
SIG_PIP3_SIGNALING_IN_B_LYMPHOCYTES	1.78	0.0113	Signaling
HSA03020_RNA_POLYMERASE	1.77	0.0074	Transcription
HSA03010_RIBOSOME	1.76	< 0.0001	Translation
PYRIMIDINE_METABOLISM	1.76	0.0055	Metabolism
INOSITOL_PHOSPHATE_METABOLISM	1.75	0.0037	Metabolism
GLYCINE_SERINE_AND_THREONINE_METABOLISM	1.72	0.0077	Metabolism
LEE_MYC_TGFA_UP	1.71	0.0036	Proliferation
5FU_RESIST_GASTRIC_UP	-1.80	< 0.0001	Chemoresistance
IDX_TSA_DN_CLUSTER6	-1.80	0.0021	Differentiation
P53HYPOXIAPATHWAY	-1.83	0.0044	Stress response
P53_BRCA1_UP	-1.85	< 0.0001	Stress response
UVC_XPCS_8HR_DN	-1.86	< 0.0001	Stress response
UVC_XPCS_ALL_DN	-1.86	< 0.0001	Stress response
CMV_24HRS_DN	-1.89	< 0.0001	Stress response
GH_AUTOCRINE_DN	-1.89	< 0.0001	Transformation
UVC_LOW_ALL_DN	-1.90	< 0.0001	Stress response
HALMOS_CEBP_DN	-1.91	< 0.0001	Proliferation
UVC_TTD-XPCS_COMMON_DN	-1.93	< 0.0001	Stress response
UVC_TTD_4HR_DN	-1.94	< 0.0001	Stress response
UVC_LOW_ALL_UP	-1.94	0.0021	Stress response
UVC_XPCS_4HR_DN	-1.95	< 0.0001	Stress response
HSA04115_P53_SIGNALING_PATHWAY	-1.96	< 0.0001	Stress response
OXSTRESS_BREASTCA_UP	-1.97	< 0.0001	Stress response
UVC_HIGH_ALL_UP	-2.10	< 0.0001	Stress response
MMS_HUMAN_LYMPH_HIGH_24HRS_UP	-2.10	< 0.0001	Chemoresistance
BLEO_HUMAN_LYMPH_HIGH_4HRS_UP	-2.16	< 0.0001	Apoptosis

Table 3 – Summary of the results of the gene-set enrichment analysis
Gene-sets are ranked by their normalized enrichment score that reflects the degree to which the gene-set is overrepresented at the extremes (top or bottom) of the entire ranked gene list yielded by microarray analysis. The normalized enrichment score (NES) accounts for different sizes of the gene-sets (Subramanian et al., 2005). Only gene-sets with an NES of at least ±1.71 are listed. Functional involvement of the gene-sets in biological processes was determined by assessment of the corresponding literature describing the experiments.

3.7 MondoA enhances survival and clonogenicity

of leukemia cells

Differentiation therapy is successfully employed to treat certain acute myeloid leukemia subtypes (Petrie et al., 2009). Accordingly, the author of this dissertation investigated whether the MondoA knockdown-mediated differentiation of ALL cells can mitigate the malignant phenotype in the present model system. Experiments addressing proliferation showed no evidence for MondoA-silencing to impact leukemia proliferation as assessed by analysis of BrdU-incorporation rates (**Figure 10A**). Consistently, MondoA knockdown did not affect cell cycle progression as pSInegative and pSImondoA Nalm6 cells exhibited similar distributions of G1, S and G2/M phases (**Figure 10B**).

Interestingly, MondoA knockdown downregulates genes sharing a significant overlap with a published expression signature of downregulated genes in primary childhood B cell lineage ALL that responded well to apoptosis-inducing therapy with glucocorticoids (**Figure 10C and Supplementary Table 2**) (Rhein et al., 2007). This observation indicates that MondoA knockdown may shift gene expression towards a signature favoring apoptosis and reducing aggressiveness of leukemia cells. In accordance, flow cytometric analysis of necrosis and apoptosis with annexin-V-PE and 7-AAD staining revealed that MondoA knockdown leads to increased rates of spontaneous cell death (**Figure 10D**). In addition, clonogenicity of the MondoA-suppressed Nalm6 cells was significantly impaired (**Figure 10E**).
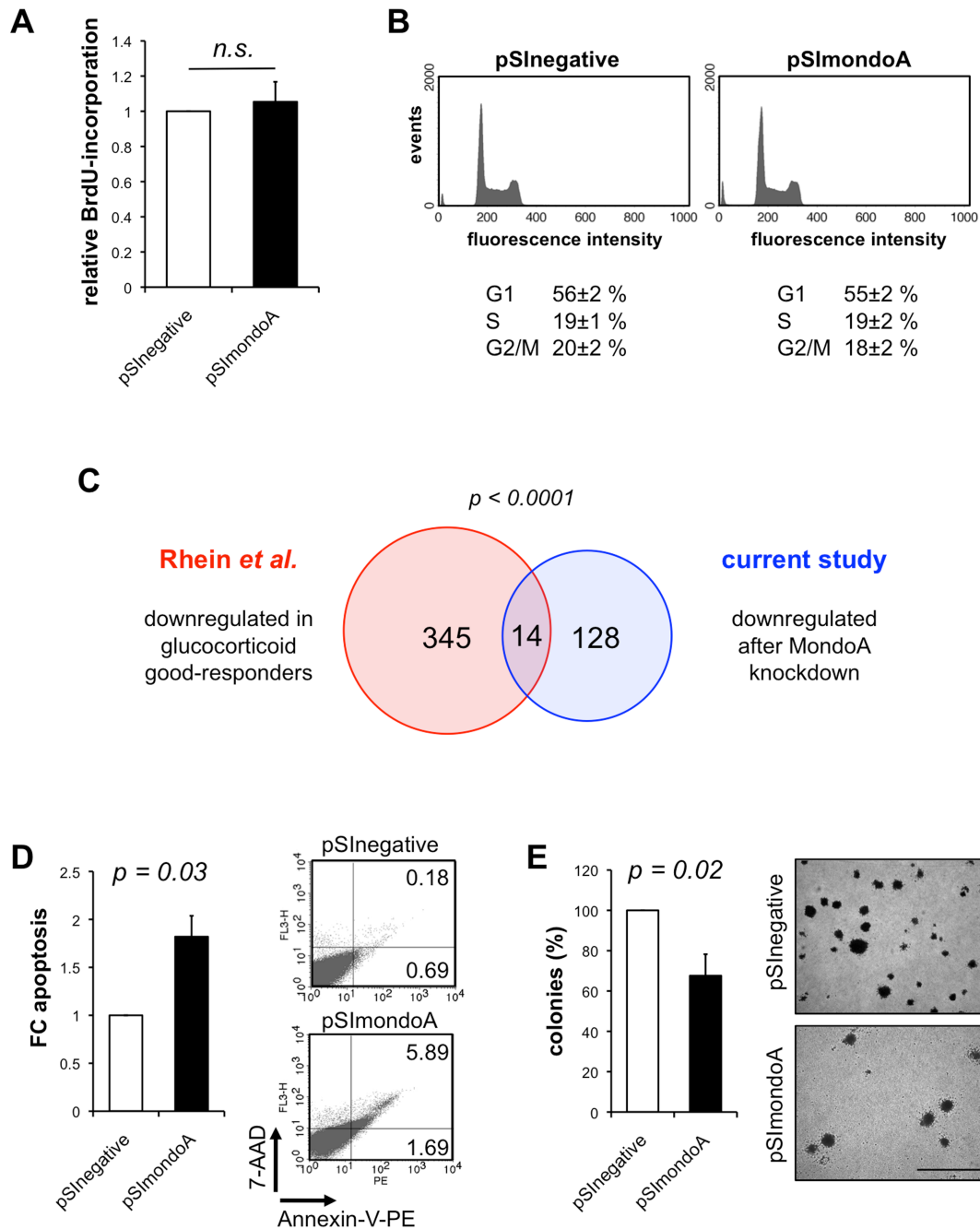
Figure 10 – MondoA promotes survival and clonogenicity of leukemia cells
(A) Analysis of proliferation with BrdU-incorporation assays of Nalm6 pSInegative and pSImondoA. Data are mean ± SEM of three independent experiments (octaplicates/group); t-test.
(B) Analysis of cell cycle phases with propidium iodide (PI) staining and flow cytometry. Images show representative measurements. Distribution of cell cycle phases is indicated below as mean ± SEM of three independent experiments.
(C) Venn diagram showing the overlap of downregulated genes in primary childhood ALL responding well to apoptosis-inducing therapy with glucocorticoids (Rhein et al., 2007) and the downregulated genes after MondoA knockdown in Nalm6 cells of the current study (see Supplementary Table 2). Fisher's exact test.

(D) Summary of results of flow cytometric measurements of apoptotic cells stained with anti-annexin-V-PE-labeled antibodies and 7-AAD. Images show representative measurements and quadrant percentages. Data are mean ± SEM of the linear fold changes assessed in two independent experiments.
(E) Analysis of clonogenicity of Nalm6 pSInegative and pSImondoA cells with methylcellulose-based colony-forming assays. Data are mean ± SEM of three independent experiments (duplicates/group). Images show a representative experiment; scale bar = 1,000 μm.

3.8 MondoA NOD-SCID mouse model

A mouse model with 13 NOD-SCID mice was designed to determine the functional role of MondoA in vivo. Several studies showed that transplantation of primary leukemia cells into NOD-SCID mice results in recipients exhibiting leukemia recapitulating the human disease (Baersch et al., 1997; Borgmann et al., 2000; Nijmeijer et al., 2001; Lock et al., 2002; Meyer et al., 2011). Eight mice were transplanted with Nalm 6 MondoA knockdown cells (pSImondoA mice), of which two had to be sacrificed during observation due to signs of infection, and five mice were transplanted with the Nalm 6 control cells (pSInegative mice).

Weight monitoring at the start, after two weeks and after five weeks of the experiment showed no significant weight loss as a sign of illness. After five weeks, mice were executed on the same day and liver, spleen, and central and peripheral lymph nodes were extracted, weighted and sent to the Department of Pathology of the Klinikum rechts der Isar for histology and immunochemistry (Dr. med. Melissa Schlitter and Prof. Dr. med. Irene Esposito) to detect leukemic infiltrates into these leukemia- typical tissues.

None out of the six pSImondoA knockdown mice, but two out of the five pSInegative control mice revealed signs of leukemic infiltrates in the liver and

the spleen (**Figure 11**). No CD10 positive cells could be observed in the peripheral blood smears. Finally, flow cytometry of peripheral blood and bone marrow samples evidenced only murine, but no human CD45 as a sign for leukemic blasts. Still, these in vivo results hint towards a shorter engraftment and time to leukemia in the pSInegative control mice.
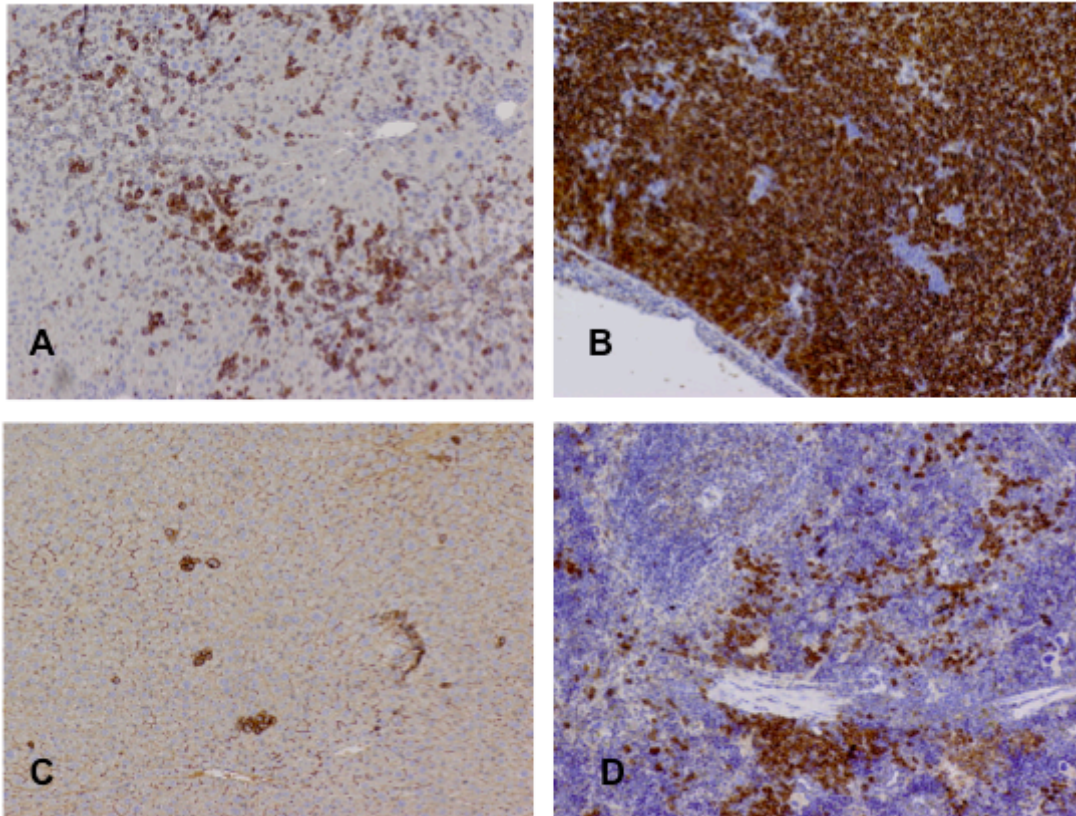
Figure 11 – leukemia infiltrates in liver and spleen in NOD-SCID mouse model
(A) pSInegative mouse 1: liver with ≈20% infiltrates of CD10 positive cells
(B) pSInegative mouse 1: spleen with ≈80-90% infiltrates of CD10 positive cells
(C) pSInegative mouse 2: liver with ≈5% infiltrates of CD10 positive cells
(D) pSInegative mouse 2: spleen with ≈10% infiltrates of CD10 positive cells
approx. 10-times magnified

3.9 MondoA correlates with hyperleukocytosis at diagnosis

In order to put MondoA in a clinical context, the author analyzed available clinical data of the 25 ALL patients of Figure 5A and B in correlation with their MondoA expression levels. No correlation with age, sex and translocations was found, but hyperleukocytosis at diagnosis, defined as over 50,000 leukocytes/ µL according to St. Jude´s Total Therapy Study XIIIB protocol criteria (Pui et al., 2004), correlated significantly with MondoA expression levels (**Figure 12**). As hyperleukocytosis reflecting high leukemic burden is a risk factor for poor prognosis (Smith et al., 1996; Möricke et al., 2010), these findings possibly hint to a contribution of MondoA to a worse clinical outcome.
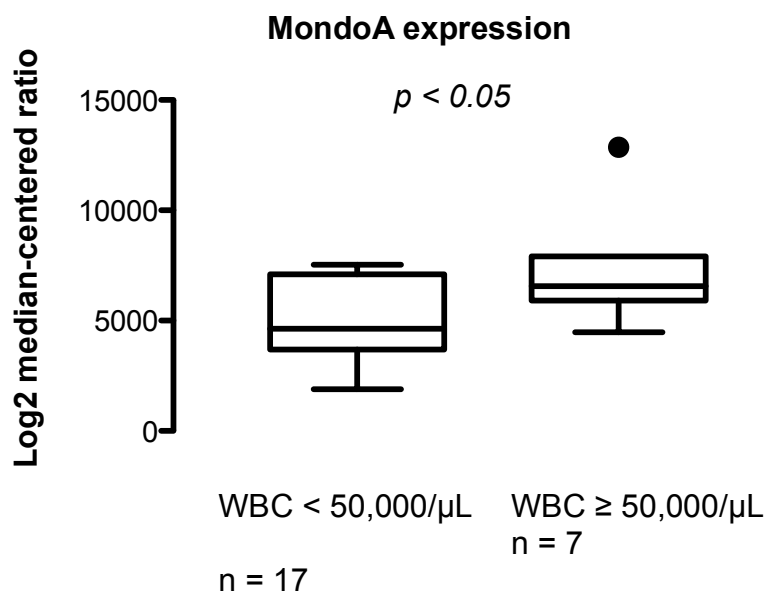
Figure 12 – MondoA expression correlates with hyperleucocytosis
Analysis of MondoA expression and white blood cell count (WBC) at diagnosis (WBC </≥ 50,000/µL) in 24 patients with primary cALL shown in Figures 5A-B. Box-plots indicate the median expression and 25th and 75th percentile, respectively. Whiskers indicate the 10th and 90th percentile. Outliers are displayed as black dots.

4 Discussion

The present dissertation aimed to determine the role of MondoA in ALL regarding glucose metabolism, growth and survival. The results provide evidence that MondoA is highly overexpressed in ALL compared to normal tissues and that MondoA promotes metabolic activity and glucose utilization of leukemia cells. Moreover, these data indicate that MondoA contributes to the maintenance of a more immature leukemia phenotype, which is linked with enhanced leukemia clonogenicity and survival.

The author shows that MondoA expression is not significantly affected by glucose availability in leukemia cells, even after prolonged time of glucose deprivation (up to 24h). In contrast, MondoA expression is suppressed by lactate, the end product of anaerobic glycolysis (Vander Heiden et al., 2009). This is in contrast to the observations of Chen *et al.* made in human MCF-7 breast cancer cells and mouse embryonic fibroblasts (MEFs) (Chen et al., 2010). In these cells, lactate treatment with higher concentrations for a longer period of time (25 mmol/L for 48h compared to 15 mmol/L for 24h used in the current study) had no effect on MondoA expression, probably due to the low basal expression of MondoA in these cells (Chen et al., 2010). However, this finding in highly MondoA overexpressing leukemia cells could mirror a negative feedback loop, which decreases the glycolytic effect of MondoA by its transcriptional downregulation when lactate accumulates.

So far, there are no reports on mutations hitting *MondoA* or other alterations that might drive its overexpression. However, in addition to this short-term regulatory effect, the author found that MondoA seems to be regulated via

DNA methylation, which almost exclusively occurs at regions of high clustering of CpG dinucleotides ("CpG-islands") and usually enables long-term gene silencing (Portela and Esteller, 2010). The author identified two conserved CpG-islands and 13 putative transcription factor binding sites within the *MondoA* promoter. Strikingly, six out of these 13 binding sites are predicted to bind RUNX1 and to flank the two CpG-islands (**Figure 6B** and **Table 2**). RUNX1 (also referred to as AML1) can block granulocytic differentiation of myeloid cells (Morishita et al., 1992) and is a major oncogene in human myeloid leukemia (Goyama et al., 2008), whose overexpression predicts poor survival (Barjesteh van Waalwijk van Doorn-Khosrovani et al., 2003; Valk et al., 2004). Of note, the fusion oncogene *TEL/AML1* (alias *ETV6/RUNX1*), which is present in 25% of childhood B cell lineage ALL (Shurtleff et al., 1995), constitutes a first-hit mutation endowing preleukemic cells with enhanced self-renewal and survival properties (Hong et al., 2008). In this regard, a regulation of MondoA by RUNX1 appears reasonable as RUNX1 and MondoA were found to be highly coexpressed in leukemia and as MondoA expression increased after treatment with zebularine, which possibly led to demethylation of the CpG-islands of the *MondoA* promoter and to increased binding of RUNX1. These observations suggest that MondoA may be a potent downstream target of RUNX1 responsible for part of the RUNX1-mediated blockage of differentiation seen in leukemia (Morishita et al., 1992; Goyama et al., 2008). Future studies now have to define the precise methylation status of the *MondoA* promoter in leukemia.

Because MondoA is involved in glucose metabolism of many different cell types (Billin and Ayer, 2006; Sans et al., 2006; Stoltzman et al., 2008), the

author first examined an association of MondoA and glucose consumption. As expected, MondoA knockdown decreased the metabolic activity and the overall glucose uptake of leukemia cells suggesting that MondoA overexpression may contribute to their highly glycolytic phenotype, which is a common feature of many cancers and known as the Warburg effect (Vander Heiden et al., 2009).

Consistently, the metabolomic analysis performed in cooperation with the Helmholtz Center Munich evidenced diminished intracellular glucose in the pSImondoA cells. Current data suggest that MondoA coordinates the utilization of glucose and glutamine by regulating the expression of thioredoxin interacting protein (TXNIP) (Stoltzman et al., 2008; Kaadige et al., 2009; Peterson and Ayer, 2012). Under physiological conditions, that is, in the presence of both glucose and glutamine, MondoA seems to repress TXNIP, resulting in a stimulation of glucose uptake (Kaadige et al., 2009). Still, as the MondoA knockdown in Nalm6 cells in this study did not enhance TXNIP expression, it can be assumed that other MondoA targets, which remain to be identified, are involved in reducing glucose uptake after MondoA knockdown.

However, the microarray and GSEA analyses in this study revealed a hitherto unexpected role of MondoA in blocking leukemia cell differentiation as indicated by the differential expression of a variety of established differentiation markers of the B cell lineage upon MondoA knockdown. Interestingly, these markers had been previously associated with growth, B cell activation and differentiation as well as survival: for instance, TGFBR2 (transforming growth factor beta receptor 2), which the author found to be transcriptionally repressed by MondoA and which others found to be

functionally antagonized by RUNX1 (Kurokawa et al., 1998), promotes cellular lineage fate decisions and terminal differentiation of many different cell types (Massagué, 2008). *DNTT* (terminal deoxynucleotidyltransterase), which is upregulated by MondoA, is expressed in normal and malignant pre-B and pre-T lymphocytes during early differentiation and contributes to generation of antigen-receptor diversity (Thai and Kearney, 2004). In addition, DNTT has a strong anti-apoptotic function as its overexpression may contribute to resistance of leukemia cells to thiopurine-based chemotherapeutics (Karim et al., 2011). Accordingly, downregulation of DNTT by MondoA knockdown may in part explain the increased rates of spontaneous apoptosis in the present model. Similarly, DDIT3 (DNA-damage-inducible transcript 3, also known as CHOP-10 and GADD153) is involved in differentiation and survival of various tissues (Maytin and Habener, 1998; Coutts et al., 1999; Pereira et al., 2004). Moreover, PDGFRA (platelet-derived growth factor receptor alpha), which is downregulated after MondoA-silencing, is frequently overexpressed in childhood ALL (Yeoh et al., 2002) and often rearranged in myeloid and lymphoid neoplasms. Besides, its inhibition by Imatinib (Gleevec®) can induce remissions, which emphasizes its oncogenic function (Vladareanu et al., 2010).

Furthermore, the author detected the upregulation of the B cell differentiation markers CD20, CD22, CD24 and CD79a upon MondoA knockdown. These findings confirmed the GSEA *in silico* prediction that MondoA overexpression maintains a more immature phenotype since these markers are usually more abundantly expressed in differentiated B cells (Chu and Arber, 2001; Fang et al., 2010; Raponi et al., 2011). In addition, enhanced CD24 expression may

promote apoptosis in pre-B cells (Taguchi et al., 2003; Ju et al., 2011) converging with the fact that MondoA knockdown in leukemia cells increases rates of spontaneous cell death and shifts gene expression toward a signature related to enhanced sensitivity of leukemia cells toward chemotherapy (GSEA, **Table 3**). Consistently, MondoA downregulation leads to decreased clonogenicity of leukemia cells and to transcriptional changes similar to those seen in ALL samples derived from patients that responded well to treatment with glucocorticoids (Rhein et al., 2007). These data suggest that MondoA overexpression may contribute to a worse outcome of ALL patients because especially more immature cells that display a leukemia stem-cell phenotype are believed to be extremely therapy-resistant and the main source of leukemic relapse (Buss and Ho, 2011). However, there is currently no drug available or under development that can specifically target MondoA.

Concerning the mouse model, several studies showed that transplantation of primary leukemia cells into NOD-SCID mice results in recipients exhibiting leukemia recapitulating the human disease (Baersch et al., 1997; Borgmann et al., 2000; Nijmeijer et al., 2001; Lock et al., 2002; Meyer et al., 2011). Meyer et al. observed that rapid development of leukemia in NOD-SCID mice engrafted with primary ALL cells is characteristic for patients with early relapse (Meyer et al., 2011). However, these studies were performed with primary leukemia cells rather than leukemia cell lines, which could explain the worse engraftment in our model. In addition, the time of observation should be prolonged, as other groups evidenced engraftment after several weeks to months (range 4-26 weeks), monitored by weekly determination of human CD45 positive cells via flow cytometry in the murine peripheral blood (Lock et

al., 2002; Bhadri et al., 2011; Meyer et al., 2011). Of note, leukemia was consistently first detected in the bone marrow and the spleen followed by the occurrence of ALL cells in the peripheral blood (Meyer et al., 2011). As such, it is not astonishing that the author could not yet detect blasts in the blood smears of the two pSInegative mice with liver and spleen infiltrates (**Figure 11**). Altogether, these *in vivo* results hint toward a shorter engraftment and time-to-leukemia in the pSInegative control mice, suggesting that high MondoA expression possibly leads to a more aggressive phenotype. Further experiments with more mice and a longer observational time should be conducted to substantiate these findings.

Interestingly, also the analysis of the available clinical data of the 25 ALL patients of Figure 5A and B hints to a worsened clinical outcome through MondoA, as hyperleukocytosis at time of diagnosis as a known risk factor for poor prognosis (Smith et al., 1996; Möricke et al., 2010) correlated with MondoA expression levels in these patients. Prospective large-scale clinical studies are now required to validate the observed correlation between MondoA expression levels and the clinical outcome of pediatric ALL patients.

5 Conclusions

57

To the author´s knowledge, this is the first report confirming that MondoA is highly overexpressed in ALL compared to normal tissue and providing evidence that MondoA not only plays a role in glucose metabolism, but also in the maintenance of a more immature leukemia phenotype, which is associated with enhanced survival and clonogenicity. These data hint to an important contribution of MondoA to leukemia aggressiveness validating MondoA as an attractive candidate for targeted treatment of ALL. Future studies will have to determine the pathways involved in regulation and functioning of MondoA and to evaluate MondoA as a potential therapeutic target and as a prognostic and/or predictive biomarker for ALL.

6 Limitations of the study and perspectives

Previous microarray studies showed that the transcription factor MondoA is highly expressed in ALL in children, but its significance in ALL had not been investigated so far. This dissertation addressed the role of MondoA in metabolism, differentiation and survival of leukemia cell lines derived from children with ALL. Still, several limitations and unresolved questions remain which need to be addressed in future studies to fully elucidate the role of MondoA in ALL.

First, the investigated cells were cell lines that have been cultured for many years and that have therefore likely acquired additional genetic mutations leading to diverse phenotypes. In addition, cell lines are mostly derived from a few surviving cells of a large pool of leukemia cells obtained from patients with a very aggressive course of the disease, possibly explaining why these cells are more capable to cope with *in vitro* culture conditions compared to leukemia cells in living patients. Accordingly, leukemia cell lines are subclones of a few cells adapted to the *in vitro* situation and may not be fully representative for the whole leukemic cell population. As a consequence, leukemia cell lines cannot fully recapitulate the true behavior of *in vivo* cells, which is why the results of this dissertation should also be verified on primary patient-derived cell culture whenever possible.

Secondly, the MondoA knockdown experiments in this study showed most of the key results. However, a constitutional knockdown is difficult to achieve in non-adherent cells such as leukemia cells, with a maximal knockdown to around 40% yielded in this study. Thus, some results may appear less

obvious and less significant as they would have had with a better knockdown of MondoA.

Furthermore, the *in vivo* part of the study was conceived rather as a pilot study, starting with 13 mice to test if engraftment is generally possible with this mouse model and if some differences in extent of disease between control and knockdown mice can be seen. Several previous studies showed that transplantation of primary leukemia cells into NOD-SCID mice results in recipients exhibiting leukemia recapitulating the human disease (Baersch et al., 1997; Borgmann et al., 2000; Nijmeijer et al., 2001; Lock et al., 2002; Meyer et al., 2011). After five weeks, only two of 11 mice (two mice had to be precociously sacrificed earlier because of signs of microbial infection) showed leukemic infiltration into the liver and spleen, both mice were part of the control group. However, it is difficult to draw any direct conclusions from such a small number of cases. Further investigations should be conducted with higher number of cases and a prolonged observation time, with optimized monitoring of disease onset, such as weekly determination of human CD45 positive cells via flow cytometry in the murine peripheral blood (see discussion).

Besides, assessing the susceptibility to chemotherapy of MondoA control versus knockdown cells *in vitro* and *in vivo* could be of clinical interest.

Finally, a broader patient study should be conceived to investigate the effect of MondoA on outcome of pediatric ALL patients. Analysis of the available clinical data of the 24 ALL patients of Figure 5A and 5B showed a correlation between MondoA expression levels and hyperleukocytosis at diagnosis as a marker for worsened outcome (Smith et al., 1996; Möricke et al., 2010).

However, no data about the patient's outcome was available, which would be useful to determine if MondoA expression plays an important role in leukemia aggressiveness not only *in vitro* as indicated by this study but also *in vivo*. This author recommends to conduct a prospective study, analyzing MondoA expression at diagnosis and at several time points during treatment, and to compare and correlate the results with established prognostic markers as MRD and the patients' outcome.

6 Summary

Acute lymphoblastic leukemia (ALL) is the most common childhood cancer, which is generally associated with good overall survival rates of around 80%. However, conventional therapies are accompanied by considerable short- and long-term toxicity. Therefore, the development of targeted therapies may be the prerequisite to reduce the toxic burden of cure. To identify novel candidates for targeted therapy, a previously performed transcriptome analysis of early pre-B cell ALL and fetal early pre-B cells (FEB) yielded a set of genes specifically overexpressed in childhood ALL. Among them MondoA was identified - a transcription factor regulating glycolysis in response to glucose availability.

The author´s objectives were to verify the preliminary microarray data, to determine possible mechanisms of MondoA regulation and to define the functional role of MondoA in leukemia cells concerning glucose metabolism, survival and differentiation, thus to investigate its potential functional role for the malignant phenotype of ALL.

The experiments described in this dissertation thesis confirm that MondoA is highly overexpressed in ALL, whereas the MondoA paralog MondoB is not expressed. The author shows that MondoA is not significantly regulated by glucose availability in leukemia cells, but by the presence of lactate. *In silico MondoA* promoter analysis identified two methylation-prone CpG-islands and six conserved binding sites for the transcription factor RUNX1. Indeed, MondoA and RUNX1 are significantly coexpressed in leukemia and experimental blockage of DNA methylation causes further induction of

MondoA. Using microarray profiling, gene-set enrichment analysis and RNA interference, this dissertation provides evidence that MondoA expression not only increases glucose catabolism, but also maintains a more immature ALL phenotype, which is associated with enhanced survival and clonogenicity of leukemia cells. The MondoA mouse model and the patient study in this work support this hypothesis.

In conclusion, these data hint to an important contribution of MondoA to leukemia aggressiveness validating MondoA as an attractive candidate for targeted treatment of ALL.

7 References

Andersson, A., Ritz, C., Lindgren, D., Edén, P., Lassen, C., Heldrup, J., Olofsson, T., Råde, J., Fontes, M., Porwit-Macdonald, A., et al. (2007). Microarray-based classification of a consecutive series of 121 childhood acute leukemias: prediction of leukemic and genetic subtype as well as of minimal residual disease status. Leukemia *21*, 1198–1203.

Baersch, G., Möllers, T., Hötte, A., Dockhorn-Dworniczak, B., Rübe, C., Ritter, J., Jürgens, H., and Vormoor, J. (1997). Good engraftment of B-cell precursor ALL in NOD-SCID mice. Klin Padiatr *209*, 178–185.

Balgobind, B.V., Van den Heuvel-Eibrink, M.M., De Menezes, R.X., Reinhardt, D., Hollink, I.H.I.M., Arentsen-Peters, S.T.J.C.M., van Wering, E.R., Kaspers, G.J.L., Cloos, J., de Bont, E.S.J.M., et al. (2011). Evaluation of gene expression signatures predictive of cytogenetic and molecular subtypes of pediatric acute myeloid leukemia. Haematologica *96*, 221–230.

Barjesteh van Waalwijk van Doorn-Khosrovani, S., Erpelinck, C., van Putten, W.L.J., Valk, P.J.M., van der Poel-van de Luytgaarde, S., Hack, R., Slater, R., Smit, E.M.E., Beverloo, H.B., Verhoef, G., et al. (2003). High EVI1 expression predicts poor survival in acute myeloid leukemia: a study of 319 de novo AML patients. Blood *101*, 837–845.

Beate Beinvogl (2010). Hochaufgereinigte CD19+CD10+ fetale B-Zellen aus Nabelschnurblut als Vergleichszellen zur pädiatrischen Akuten Lymphoblastischen Leukämie (cALL) identifizieren eine neue Expressionssignatur des malignen Phänotyps.

Beillard, E., Pallisgaard, N., van der Velden, V.H.J., Bi, W., Dee, R., van der Schoot, E., Delabesse, E., Macintyre, E., Gottardi, E., Saglio, G., et al. (2003). Evaluation of candidate control genes for diagnosis and residual disease detection in leukemic patients using "real-time" quantitative reverse-transcriptase polymerase chain reaction (RQ-PCR) - a Europe against cancer program. Leukemia *17*, 2474–2486.

Bhadri, V.A., Cowley, M.J., Kaplan, W., Trahair, T.N., and Lock, R.B. (2011). Evaluation of the NOD/SCID xenograft model for glucocorticoid-regulated gene expression in childhood B-cell precursor acute lymphoblastic leukemia. BMC Genomics *12*, 565.

Billin, A.N., and Ayer, D.E. (2006). The Mlx network: evidence for a parallel Max-like transcriptional network that regulates energy metabolism. Curr. Top. Microbiol. Immunol. *302*, 255–278.

Billin, A.N., Eilers, A.L., Coulter, K.L., Logan, J.S., and Ayer, D.E. (2000). MondoA, a novel basic helix-loop-helix-leucine zipper transcriptional activator that constitutes a positive branch of a max-like network. Mol. Cell. Biol. *20*, 8845–8854.

Bleyer, W.A. (1988). Central nervous system leukemia. Pediatr. Clin. North Am. *35*, 789–814.

Borgmann, A., Baldy, C., von Stackelberg, A., Beyermann, B., Fichtner, I., Nürnberg, P., and Henze, G. (2000). Childhood all blasts retain phenotypic and genotypic characteristics upon long-term serial passage in NOD/SCID mice. Pediatr Hematol Oncol *17*, 635–650.

Bourquin, J.P., and Izraeli, S. (2010). Where can biology of childhood ALL be attacked by new compounds? Cancer Treat. Rev. *36*, 298–306.

Brunning RD et al. Precursor B lymphoblastic leukaemia/lymphoblastic lymphoma.

In: WHO Classification of Tumours. Pathology and Genetics of Tumours of Haematopoietic and Lymphoid Tissues, Jaffe ES et al., IARC Press, Lyon 2001 p.111.

Bürger, B., Beier, R., Zimmermann, M., Beck, J.D., Reiter, A., and Schrappe, M. (2005). Osteonecrosis: a treatment related toxicity in childhood acute lymphoblastic leukemia (ALL)--experiences from trial ALL-BFM 95. Pediatr Blood Cancer *44*, 220–225.

Buss, E.C., and Ho, A.D. (2011). Leukemia stem cells. Int. J. Cancer *129*, 2328–2336.

Cadenas, C., Franckenstein, D., Schmidt, M., Gehrmann, M., Hermes, M., Geppert, B., Schormann, W., Maccoux, L.J., Schug, M., Schumann, A., et al. (2010). Role of thioredoxin reductase 1 and thioredoxin interacting protein in prognosis of breast cancer. Breast Cancer Res. *12*, R44.

Cario, G., Stanulla, M., Fine, B.M., Teuffel, O., Neuhoff, N.V., Schrauder, A., Flohr, T., Schäfer, B.W., Bartram, C.R., Welte, K., et al. (2005). Distinct gene expression profiles determine molecular treatment response in childhood acute lymphoblastic leukemia. Blood *105*, 821–826.

Carroll, W.L., Bhojwani, D., Min, D.-J., Raetz, E., Relling, M., Davies, S., Downing, J.R., Willman, C.L., and Reed, J.C. (2003). Pediatric acute lymphoblastic leukemia. Hematology Am Soc Hematol Educ Program 102–131.

Chekmenev, D.S., Haid, C., and Kel, A.E. (2005). P-Match: transcription factor binding site search by combining patterns and weight matrices. Nucleic Acids Res. *33*, W432–437.

Chen, J.L.-Y., Merl, D., Peterson, C.W., Wu, J., Liu, P.Y., Yin, H., Muoio, D.M., Ayer, D.E., West, M., and Chi, J.-T. (2010). Lactic acidosis triggers starvation response with paradoxical induction of TXNIP through MondoA. PLoS Genet. *6*,.

Chu, P.G., and Arber, D.A. (2001). CD79: a review. Appl. Immunohistochem. Mol. Morphol. *9*, 97–106.

Conter, V., Bartram, C.R., Valsecchi, M.G., Schrauder, A., Panzer-Grümayer, R., Möricke, A., Aricò, M., Zimmermann, M., Mann, G., De Rossi, G., et al. (2010). Molecular response to treatment redefines all prognostic factors in children and adolescents with B-cell precursor acute lymphoblastic leukemia: results in 3184 patients of the AIEOP-BFM ALL 2000 study. Blood *115*, 3206–3214.

Coutts, M., Cui, K., Davis, K.L., Keutzer, J.C., and Sytkowski, A.J. (1999). Regulated expression and functional role of the transcription factor CHOP (GADD153) in erythroid growth and differentiation. Blood *93*, 3369–3378.

Eden, T. (2010). Aetiology of childhood leukaemia. Cancer Treat. Rev. *36*, 286–297.

Eilers, A.L., Sundwall, E., Lin, M., Sullivan, A.A., and Ayer, D.E. (2002). A novel heterodimerization domain, CRM1, and 14-3-3 control subcellular localization of the MondoA-Mlx heterocomplex. Mol. Cell. Biol. *22*, 8514–8526.

Eisen, M.B., Spellman, P.T., Brown, P.O., and Botstein, D. (1998). Cluster analysis and display of genome-wide expression patterns. Proc. Natl. Acad. Sci. U.S.A. *95*, 14863–14868.

Fang, X., Zheng, P., Tang, J., and Liu, Y. (2010). CD24: from A to Z. Cell. Mol. Immunol. *7*, 100–103.

Ferrando, A.A., and Look, A.T. (2003). Gene expression profiling in T-cell acute lymphoblastic leukemia. Semin. Hematol. *40*, 274–280.

Gale, K.B., Ford, A.M., Repp, R., Borkhardt, A., Keller, C., Eden, O.B., and Greaves, M.F. (1997). Backtracking leukemia to birth: identification of clonotypic gene fusion sequences in neonatal blood spots. Proc. Natl. Acad. Sci. U.S.A. *94*, 13950–13954.

Gaynon, P.S., and Carrel, A.L. (1999). Glucocorticosteroid therapy in childhood acute lymphoblastic leukemia. Adv. Exp. Med. Biol. *457*, 593–605.

Ge, X., Yamamoto, S., Tsutsumi, S., Midorikawa, Y., Ihara, S., Wang, S.M., and Aburatani, H. (2005). Interpreting expression profiles of cancers by genome-wide survey of breadth of expression in normal tissues. Genomics *86*, 127–141.

Goldberg, S.F., Miele, M.E., Hatta, N., Takata, M., Paquette-Straub, C., Freedman, L.P., and Welch, D.R. (2003). Melanoma metastasis suppression by chromosome 6: evidence for a pathway regulated by CRSP3 and TXNIP. Cancer Res. *63*, 432–440.

Goyama, S., Yamamoto, G., Shimabe, M., Sato, T., Ichikawa, M., Ogawa, S., Chiba, S., and Kurokawa, M. (2008). Evi-1 is a critical regulator for hematopoietic stem cells and transformed leukemic cells. Cell Stem Cell *3*, 207–220.

Greaves, M. (2006). Infection, immune responses and the aetiology of childhood leukaemia. Nat. Rev. Cancer *6*, 193–203.

Greaves, M.F., and Wiemels, J. (2003). Origins of chromosome translocations in childhood leukaemia. Nat. Rev. Cancer *3*, 639–649.

Grunewald, T.G., Pasedag, S.M., and Butt, E. (2009). Cell Adhesion and Transcriptional Activity - Defining the Role of the Novel Protooncogene LPP. Transl Oncol *2*, 107–116.

Grunewald, T.G.P., Diebold, I., Esposito, I., Plehm, S., Hauer, K., Thiel, U., da Silva-Buttkus, P., Neff, F., Unland, R., Müller-Tidow, C., et al. (2012). STEAP1 Is Associated with the Invasive and Oxidative Stress Phenotype of Ewing Tumors. Mol. Cancer Res. *10*, 52–65.

Haferlach, T., Kohlmann, A., Wieczorek, L., Basso, G., Kronnie, G.T., Béné, M.-C., De Vos, J., Hernández, J.M., Hofmann, W.-K., Mills, K.I., et al. (2010). Clinical utility of microarray-based gene expression profiling in the diagnosis and subclassification of leukemia: report from the International Microarray Innovations in Leukemia Study Group. J. Clin. Oncol. *28*, 2529–2537.

Han, S.H., Jeon, J.H., Ju, H.R., Jung, U., Kim, K.Y., Yoo, H.S., Lee, Y.H., Song, K.S., Hwang, H.M., Na, Y.S., et al. (2003). VDUP1 upregulated by TGF-beta1 and 1,25-dihydorxyvitamin D3 inhibits tumor cell growth by blocking cell-cycle progression. Oncogene *22*, 4035–4046.

Hong, D., Gupta, R., Ancliff, P., Atzberger, A., Brown, J., Soneji, S., Green, J., Colman, S., Piacibello, W., Buckle, V., et al. (2008). Initiating and cancer-propagating cells in TEL-AML1-associated childhood leukemia. Science *319*, 336–339.

Howard W. Robinson, and Corinne G. Hogden (1941). The influence of serum proteins on the spectrophotometric absorption curve of phenol red in a phosphate buffer mixture. The Journal of Biological Chemistry 239–254.

Hui, S.T.Y., Andres, A.M., Miller, A.K., Spann, N.J., Potter, D.W., Post, N.M., Chen, A.Z., Sachithanantham, S., Jung, D.Y., Kim, J.K., et al. (2008). Txnip balances metabolic and growth signaling via PTEN disulfide reduction. Proc. Natl. Acad. Sci. U.S.A. *105*, 3921–3926.

Iizuka, K., Bruick, R.K., Liang, G., Horton, J.D., and Uyeda, K. (2004). Deficiency of carbohydrate response element-binding protein (ChREBP) reduces lipogenesis as well as glycolysis. Proc. Natl. Acad. Sci. U.S.A. *101*, 7281–7286.

Ingram, L.C., Fairclough, D.L., Furman, W.L., Sandlund, J.T., Kun, L.E., Rivera, G.K.,

and Pui, C.H. (1991). Cranial nerve palsy in childhood acute lymphoblastic leukemia and non-Hodgkin's lymphoma. Cancer *67*, 2262–2268.

Ishii, S., Iizuka, K., Miller, B.C., and Uyeda, K. (2004). Carbohydrate response element binding protein directly promotes lipogenic enzyme gene transcription. Proc. Natl. Acad. Sci. U.S.A. *101*, 15597–15602.

Islaih, M., Li, B., Kadura, I.A., Reid-Hubbard, J.L., Deahl, J.T., Altizer, J.L., Watson, D.E., and Newton, R.K. (2004). Comparison of gene expression changes induced in mouse and human cells treated with direct-acting mutagens. Environ. Mol. Mutagen. *44*, 401–419.

Ju, J., Jang, K., Lee, K.-M., Kim, M., Kim, J., Yi, J.Y., Noh, D.-Y., and Shin, I. (2011). CD24 enhances DNA damage-induced apoptosis by modulating NF-κB signaling in CD44-expressing breast cancer cells. Carcinogenesis *32*, 1474–1483.

Kaadige, M.R., Elgort, M.G., and Ayer, D.E. (2010). Coordination of glucose and glutamine utilization by an expanded Myc network. Transcription *1*, 36–40.

Kaadige, M.R., Looper, R.E., Kamalanaadhan, S., and Ayer, D.E. (2009). Glutamine-dependent anapleurosis dictates glucose uptake and cell growth by regulating MondoA transcriptional activity. Proc. Natl. Acad. Sci. U.S.A. *106*, 14878–14883.

Karim, H., Hashemi, J., Larsson, C., Moshfegh, A., Fotoohi, A.K., and Albertioni, F. (2011). The pattern of gene expression and gene dose profiles of 6-Mercaptopurine- and 6-Thioguanine-resistant human leukemia cells. Biochem. Biophys. Res. Commun. *411*, 156–161.

Kaspers, G.J., Pieters, R., Van Zantwijk, C.H., Van Wering, E.R., Van Der Does-Van Den Berg, A., and Veerman, A.J. (1998). Prednisolone resistance in childhood acute lymphoblastic leukemia: vitro-vivo correlations and cross-resistance to other drugs. Blood *92*, 259–266.

Kim, S.Y., Suh, H.-W., Chung, J.W., Yoon, S.-R., and Choi, I. (2007). Diverse functions of VDUP1 in cell proliferation, differentiation, and diseases. Cell. Mol. Immunol. *4*, 345–351.

Kinlen, L. (1988). Evidence for an infective cause of childhood leukaemia: comparison of a Scottish new town with nuclear reprocessing sites in Britain. Lancet *2*, 1323–1327.

Kuang, S.-Q., Tong, W.-G., Yang, H., Lin, W., Lee, M.K., Fang, Z.H., Wei, Y., Jelinek, J., Issa, J.-P., and Garcia-Manero, G. (2008). Genome-wide identification of aberrantly methylated promoter associated CpG islands in acute lymphocytic leukemia. Leukemia *22*, 1529–1538.

Kurokawa, M., Mitani, K., Irie, K., Matsuyama, T., Takahashi, T., Chiba, S., Yazaki, Y., Matsumoto, K., and Hirai, H. (1998). The oncoprotein Evi-1 represses TGF-beta signalling by inhibiting Smad3. Nature *394*, 92–96.

Lauten, M., Stanulla, M., Zimmermann, M., Welte, K., Riehm, H., and Schrappe, M. (2001). Clinical outcome of patients with childhood acute lymphoblastic leukaemia and an initial leukaemic blood blast count of less than 1000 per microliter. Klin Padiatr *213*, 169–174.

Lock, R.B., Liem, N., Farnsworth, M.L., Milross, C.G., Xue, C., Tajbakhsh, M., Haber, M., Norris, M.D., Marshall, G.M., and Rice, A.M. (2002). The nonobese diabetic/severe combined immunodeficient (NOD/SCID) mouse model of childhood acute lymphoblastic leukemia reveals intrinsic differences in biologic characteristics at diagnosis and relapse. Blood *99*, 4100–4108.

Ma, L., Nikolas G Tsatsos, and Towle, H.C. (2005). Direct role of ChREBP.Mlx in

regulating hepatic glucose-responsive genes. J. Biol. Chem. *280*, 12019–12027.

Margolin JF et al. Acute Lymphoblastic Leukemia. In: Principles and Practice of Pediatric Oncology, Pizzo PA et al., Lippincott-Raven, Philadelphia 2001 p.489.

Massagué, J. (2008). TGFbeta in Cancer. Cell *134*, 215–230.

Maytin, E.V., and Habener, J.F. (1998). Transcription factors C/EBP alpha, C/EBP beta, and CHOP (Gadd153) expressed during the differentiation program of keratinocytes in vitro and in vivo. J. Invest. Dermatol. *110*, 238–246.

McNally, R.J.Q., and Eden, T.O.B. (2004). An infectious aetiology for childhood acute leukaemia: a review of the evidence. Br. J. Haematol. *127*, 243–263.

Meyer, L.H., Eckhoff, S.M., Queudeville, M., Kraus, J.M., Giordan, M., Stursberg, J., Zangrando, A., Vendramini, E., Möricke, A., Zimmermann, M., et al. (2011). Early relapse in all is identified by time to leukemia in NOD/SCID mice and is characterized by a gene signature involving survival pathways. Cancer Cell *19*, 206–217.

Möricke, A., Zimmermann, M., Reiter, A., Henze, G., Schrauder, A., Gadner, H., Ludwig, W.D., Ritter, J., Harbott, J., Mann, G., et al. (2010). Long-term results of five consecutive trials in childhood acute lymphoblastic leukemia performed by the ALL-BFM study group from 1981 to 2000. Leukemia *24*, 265–284.

Morishita, K., Parganas, E., Matsugi, T., and Ihle, J.N. (1992). Expression of the Evi-1 zinc finger gene in 32Dc13 myeloid cells blocks granulocytic differentiation in response to granulocyte colony-stimulating factor. Mol. Cell. Biol. *12*, 183–189.

Muoio, D.M. (2007). TXNIP links redox circuitry to glucose control. Cell Metab. *5*, 412–414.

Murphy, K.M., Travers, P., and Walport, M. Janeway´s immunobiology (Taylor & Francis).

Nijmeijer, B.A., Mollevanger, P., van Zelderen-Bhola, S.L., Kluin-Nelemans, H.C., Willemze, R., and Falkenburg, J.H. (2001). Monitoring of engraftment and progression of acute lymphoblastic leukemia in individual NOD/SCID mice. Exp. Hematol. *29*, 322–329.

Parikh, H., Carlsson, E., Chutkow, W.A., Johansson, L.E., Storgaard, H., Poulsen, P., Saxena, R., Ladd, C., Schulze, P.C., Mazzini, M.J., et al. (2007). TXNIP regulates peripheral glucose metabolism in humans. PLoS Med. *4*, e158.

Pereira, R.C., Delany, A.M., and Canalis, E. (2004). CCAAT/enhancer binding protein homologous protein (DDIT3) induces osteoblastic cell differentiation. Endocrinology *145*, 1952–1960.

Peterson, C.W., and Ayer, D.E. (2012). An extended Myc network contributes to glucose homeostasis in cancer and diabetes. Front. Biosci. *17*, 2206–2223.

Peterson, C.W., Stoltzman, C.A., Sighinolfi, M.P., Han, K.-S., and Ayer, D.E. (2010). Glucose controls nuclear accumulation, promoter binding, and transcriptional activity of the MondoA-Mlx heterodimer. Mol. Cell. Biol. *30*, 2887–2895.

Petrie, K., Zelent, A., and Waxman, S. (2009). Differentiation therapy of acute myeloid leukemia: past, present and future. Curr. Opin. Hematol. *16*, 84–91.

Portela, A., and Esteller, M. (2010). Epigenetic modifications and human disease. Nat. Biotechnol. *28*, 1057–1068.

Pui, C.-H., Carroll, W.L., Meshinchi, S., and Arceci, R.J. (2011). Biology, risk stratification, and therapy of pediatric acute leukemias: an update. J. Clin. Oncol. *29*, 551–565.

Pui, C.-H., and Evans, W.E. (2006). Treatment of acute lymphoblastic leukemia. N. Engl. J. Med. *354*, 166–178.

Pui, C.-H., Robison, L.L., and Look, A.T. (2008). Acute lymphoblastic leukaemia. Lancet *371*, 1030–1043.

Pui, C.-H., Sandlund, J.T., Pei, D., Campana, D., Rivera, G.K., Ribeiro, R.C., Rubnitz, J.E., Razzouk, B.I., Howard, S.C., Hudson, M.M., et al. (2004). Improved outcome for children with acute lymphoblastic leukemia: results of Total Therapy Study XIIIB at St Jude Children's Research Hospital. Blood *104*, 2690–2696.

Ramalho-Santos, M., Yoon, S., Matsuzaki, Y., Mulligan, R.C., and Melton, D.A. (2002). "Stemness": transcriptional profiling of embryonic and adult stem cells. Science *298*, 597–600.

Raponi, S., De Propris, M.S., Intoppa, S., Milani, M.L., Vitale, A., Elia, L., Perbellini, O., Pizzolo, G., Foá, R., and Guarini, A. (2011). Flow cytometric study of potential target antigens (CD19, CD20, CD22, CD33) for antibody-based immunotherapy in acute lymphoblastic leukemia: analysis of 552 cases. Leuk. Lymphoma *52*, 1098–1107.

Rhein, P., Scheid, S., Ratei, R., Hagemeier, C., Seeger, K., Kirschner-Schwabe, R., Moericke, A., Schrappe, M., Spang, R., Ludwig, W.-D., et al. (2007). Gene expression shift towards normal B cells, decreased proliferative capacity and distinct surface receptors characterize leukemic blasts persisting during induction therapy in childhood acute lymphoblastic leukemia. Leukemia *21*, 897–905.

Rhodes, D.R., Yu, J., Shanker, K., Deshpande, N., Varambally, R., Ghosh, D., Barrette, T., Pandey, A., and Chinnaiyan, A.M. (2004). Large-scale meta-analysis of cancer microarray data identifies common transcriptional profiles of neoplastic transformation and progression. Proc. Natl. Acad. Sci. U.S.A. *101*, 9309–9314.

Richter, G., Hattenhorst, U.E., Roessler, S., Staege, M.S., Hansen, G., and Burdach, S. (2005). Transcriptome Analysis of Pediatric cALL Versus Normal Fetal B Cells Reveals a Novel Signature of the Malignant Phenotype. ASH Annual Meeting Abstracts *106*, 4352.

Ross, M.E., Zhou, X., Song, G., Shurtleff, S.A., Girtman, K., Williams, W.K., Liu, H.-C., Mahfouz, R., Raimondi, S.C., Lenny, N., et al. (2003). Classification of pediatric acute lymphoblastic leukemia by gene expression profiling. Blood *102*, 2951–2959.

Roth, R.B., Hevezi, P., Lee, J., Willhite, D., Lechner, S.M., Foster, A.C., and Zlotnik, A. (2006). Gene expression analyses reveal molecular relationships among 20 regions of the human CNS. Neurogenetics *7*, 67–80.

Samudio, I., Fiegl, M., and Andreeff, M. (2009). Mitochondrial uncoupling and the Warburg effect: molecular basis for the reprogramming of cancer cell metabolism. Cancer Res. *69*, 2163–2166.

Samudio, I., Fiegl, M., McQueen, T., Clise-Dwyer, K., and Andreeff, M. (2008). The warburg effect in leukemia-stroma cocultures is mediated by mitochondrial uncoupling associated with uncoupling protein 2 activation. Cancer Res. *68*, 5198–5205.

Sans, C.L., Satterwhite, D.J., Stoltzman, C.A., Breen, K.T., and Ayer, D.E. (2006). MondoA-Mlx heterodimers are candidate sensors of cellular energy status: mitochondrial localization and direct regulation of glycolysis. Mol. Cell. Biol. *26*, 4863–4871.

Schrappe, M., Camitta, B., Pui, C.H., Eden, T., Gaynon, P., Gustafsson, G., Janka-Schaub, G.E., Kamps, W., Masera, G., Sallan, S., et al. (2000). Long-term results of large prospective trials in childhood acute lymphoblastic leukemia. Leukemia *14*,

2193–2194.

Shin, D., Jeon, J.-H., Jeong, M., Suh, H.-W., Kim, S., Kim, H.-C., Moon, O.-S., Kim, Y.-S., Chung, J.W., Yoon, S.R., et al. (2008). VDUP1 mediates nuclear export of HIF1alpha via CRM1-dependent pathway. Biochim. Biophys. Acta *1783*, 838–848.

Shurtleff, S.A., Buijs, A., Behm, F.G., Rubnitz, J.E., Raimondi, S.C., Hancock, M.L., Chan, G.C., Pui, C.H., Grosveld, G., and Downing, J.R. (1995). TEL/AML1 fusion resulting from a cryptic t(12;21) is the most common genetic lesion in pediatric ALL and defines a subgroup of patients with an excellent prognosis. Leukemia *9*, 1985–1989.

Silverman, L.B., and Sallan, S.E. (2003). Newly diagnosed childhood acute lymphoblastic leukemia: update on prognostic factors and treatment. Curr. Opin. Hematol. *10*, 290–296.

Sinigaglia, R., Gigante, C., Bisinella, G., Varotto, S., Zanesco, L., and Turra, S. (2008). Musculoskeletal manifestations in pediatric acute leukemia. J Pediatr Orthop *28*, 20–28.

Sloan, E.J., and Ayer, D.E. (2010). Myc, mondo, and metabolism. Genes Cancer *1*, 587–596.

Smith, M., Arthur, D., Camitta, B., Carroll, A.J., Crist, W., Gaynon, P., Gelber, R., Heerema, N., Korn, E.L., Link, M., et al. (1996). Uniform approach to risk classification and treatment assignment for children with acute lymphoblastic leukemia. J. Clin. Oncol. *14*, 18–24.

Stoltzman, C.A., Kaadige, M.R., Peterson, C.W., and Ayer, D.E. (2011). MondoA senses non-glucose sugars: regulation of thioredoxin-interacting protein (TXNIP) and the hexose transport curb. J. Biol. Chem. *286*, 38027–38034.

Stoltzman, C.A., Peterson, C.W., Breen, K.T., Muoio, D.M., Billin, A.N., and Ayer, D.E. (2008). Glucose sensing by MondoA:Mlx complexes: a role for hexokinases and direct regulation of thioredoxin-interacting protein expression. Proc. Natl. Acad. Sci. U.S.A. *105*, 6912–6917.

Sturn, A., Quackenbush, J., and Trajanoski, Z. (2002). Genesis: cluster analysis of microarray data. Bioinformatics *18*, 207–208.

Subramanian, A., Tamayo, P., Mootha, V.K., Mukherjee, S., Ebert, B.L., Gillette, M.A., Paulovich, A., Pomeroy, S.L., Golub, T.R., Lander, E.S., et al. (2005). Gene set enrichment analysis: a knowledge-based approach for interpreting genome-wide expression profiles. Proc. Natl. Acad. Sci. U.S.A. *102*, 15545–15550.

Taguchi, T., Kiyokawa, N., Mimori, K., Suzuki, T., Sekino, T., Nakajima, H., Saito, M., Katagiri, Y.U., Matsuo, N., Matsuo, Y., et al. (2003). Pre-B cell antigen receptor-mediated signal inhibits CD24-induced apoptosis in human pre-B cells. J. Immunol. *170*, 252–260.

Taylor, K.H., Pena-Hernandez, K.E., Davis, J.W., Arthur, G.L., Duff, D.J., Shi, H., Rahmatpanah, F.B., Sjahputera, O., and Caldwell, C.W. (2007). Large-scale CpG methylation analysis identifies novel candidate genes and reveals methylation hotspots in acute lymphoblastic leukemia. Cancer Res. *67*, 2617–2625.

Thai, T.-H., and Kearney, J.F. (2004). Distinct and opposite activities of human terminal deoxynucleotidyltransferase splice variants. J. Immunol. *173*, 4009–4019.

Tong, X., Zhao, F., Mancuso, A., Gruber, J.J., and Thompson, C.B. (2009). The glucose-responsive transcription factor ChREBP contributes to glucose-dependent anabolic synthesis and cell proliferation. Proc. Natl. Acad. Sci. U.S.A. *106*, 21660–21665.

Tusher, V.G., Tibshirani, R., and Chu, G. (2001). Significance analysis of microarrays applied to the ionizing radiation response. Proc. Natl. Acad. Sci. U.S.A. *98*, 5116–5121.

Uehara, E., Takeuchi, S., Tasaka, T., Matsuhashi, Y., Yang, Y., Fujita, M., Tamura, T., Nagai, M., and Koeffler, H.P. (2003). Aberrant methylation in promoter-associated CpG islands of multiple genes in therapy-related leukemia. Int. J. Oncol. *23*, 693–696.

Uwe E. Hattenhorst (2003). Untersuchung der differentiellen Genexpression mit DNA-Microarrays bei Akuter Lymphoblastischer Leukämie im Vergleich mit normalen B-Lymphozyten.

Valk, P.J.M., Verhaak, R.G.W., Beijen, M.A., Erpelinck, C.A.J., Barjesteh van Waalwijk van Doorn-Khosrovani, S., Boer, J.M., Beverloo, H.B., Moorhouse, M.J., van der Spek, P.J., Löwenberg, B., et al. (2004). Prognostically useful gene-expression profiles in acute myeloid leukemia. N. Engl. J. Med. *350*, 1617–1628.

Vander Heiden, M.G., Cantley, L.C., and Thompson, C.B. (2009). Understanding the Warburg effect: the metabolic requirements of cell proliferation. Science *324*, 1029–1033.

Vladareanu, A.M., Müller-Tidow, C., Bumbea, H., and Radesi, S. (2010). Molecular markers guide diagnosis and treatment in Philadelphia chromosome-negative myeloproliferative disorders (Review). Oncol. Rep. *23*, 595–604.

WARBURG, O. (1956). On the origin of cancer cells. Science *123*, 309–314.

Wiemels, J.L., Cazzaniga, G., Daniotti, M., Eden, O.B., Addison, G.M., Masera, G., Saha, V., Biondi, A., and Greaves, M.F. (1999a). Prenatal origin of acute lymphoblastic leukaemia in children. Lancet *354*, 1499–1503.

Wiemels, J.L., Ford, A.M., Van Wering, E.R., Postma, A., and Greaves, M. (1999b). Protracted and variable latency of acute lymphoblastic leukemia after TEL-AML1 gene fusion in utero. Blood *94*, 1057–1062.

Willenbrock, H., Juncker, A.S., Schmiegelow, K., Knudsen, S., and Ryder, L.P. (2004). Prediction of immunophenotype, treatment response, and relapse in childhood acute lymphoblastic leukemia using DNA microarrays. Leukemia *18*, 1270–1277.

Yeoh, E.-J., Ross, M.E., Shurtleff, S.A., Williams, W.K., Patel, D., Mahfouz, R., Behm, F.G., Raimondi, S.C., Relling, M.V., Patel, A., et al. (2002). Classification, subtype discovery, and prediction of outcome in pediatric acute lymphoblastic leukemia by gene expression profiling. Cancer Cell *1*, 133–143.

.

8 Appendix

8.1 Supplementary data

8.1.1 Supplementary Table 1. List of 191 differentially regulated genes after MondoA-silencing in Nalm6 leukemia cells (GSE33967). Genes that have been selected for validation by qRT-PCR are marked in bold font. Expression values were log2 transformed. T-Test.

Probe set ID	Gene Symbol	Gene Description	log2 FC	*p* value
8066117	SAMHD1	SAM domain and HD domain 1	3.15	0.0064
7920291	S100A16	S100 calcium binding protein A16	2.8	0.0096
8166049	PRPS2	Phosphoribosyl pyrophosphate synthetase 2	2.27	0.0355
8171896	CXorf21	Chromosome X open reading frame 21	1.76	0.0066
7977319	PLD4	Phospholipase D family, member 4	1.53	0.0114
8033987	ICAM3	Intercellular adhesion molecule 3	1.47	0.001
7906786	FCRLA	Fc receptor-like A	1.42	0.0059
8027837	**CD22**	**CD22 molecule**	**1.29**	**0.0339**
8078350	**TGFBR2**	**Transforming growth factor, beta receptor II (70/80kDa)**	**1.17**	**0.0135**
7948332	LPXN	Leupaxin	1.13	0.0151
8053417	CAPG	Capping protein (actin filament), gelsolin-like	1.08	0.0264
7997453	PLCG2	Phospholipase C, gamma 2 (phosphatidylinositol-specific)	1.02	0.0363
7917954	FRRS1	Ferric-chelate reductase 1	1.01	0.0382
8043725	ZAP70	Zeta-chain (TCR) associated protein kinase 70kDa	0.99	0.0043
8145977	PLEKHA2	Pleckstrin homology domain containing, family A (phosphoinositide binding specific) member 2	0.95	0.044
8029136	**CD79A**	**CD79a molecule, immunoglobulin-associated alpha**	**0.92**	**0.0334**
8166219	SYAP1	Synapse associated protein 1, SAP47 homolog (Drosophila)	0.85	0.0267
7912701	FAM131C	Family with sequence similarity 131, member C	0.8	0.0405
7953878	CLEC2D	C-type lectin domain family 2, member D	0.8	0.0133
8076393	CENPM	Centromere protein M	0.78	0.0211
8006325	SUZ12	Suppressor of zeste 12 homolog (Drosophila)	0.78	0.0215
8133202	TYW1	tRNA-yW synthesizing protein 1 homolog (S. cerevisiae)	0.76	0.0373
8180078	HLA-DMB	Major histocompatibility complex, class II, DM beta	0.76	0.0036
8031238	LILRB4	Leukocyte immunoglobulin-like receptor, subfamily B (with TM and ITIM domains), member 4	0.75	0.0136
8104163	LRRC14B	Leucine rich repeat containing 14B	0.74	0.0005
8106771	NBPF22P	Neuroblastoma breakpoint family, member 22 (pseudogene)	0.71	0.0425
8102988	GYPE	Glycophorin E (MNS blood group)	0.69	0.0069
7924351	EPRS	Glutamyl-prolyl-tRNA synthetase	0.69	0.0304
8065868	EIF6	Eukaryotic translation initiation factor 6	0.64	0.0252
7977786	SLC7A7	Solute carrier family 7 (cationic amino acid transporter, y+ system), member 7	0.64	0.0274
8138151	MGC72080	MGC72080 pseudogene	0.62	0.032
7926506	CACNB2	Calcium channel, voltage-dependent, beta 2 subunit	0.62	0.0224
7932160	FAM107B	Family with sequence similarity 107, member B	0.6	0.0414
7936891	METTL10	Methyltransferase like 10	0.6	0.0427
8076690	C22orf9	Chromosome 22 open reading frame 9	0.59	0.026

8152867	ASAP1	ArfGAP with SH3 domain, ankyrin repeat and PH domain 1	0.58	0.038
8135363	PIK3CG	Phosphoinositide-3-kinase, catalytic, gamma polypeptide	0.58	0.015
8108861	NDFIP1	Nedd4 family interacting protein 1	0.56	0.0297
8053797	LOC400986	Protein immuno-reactive with anti-PTH polyclonal antibodies	0.56	0.042
8068697	MX2	Myxovirus (influenza virus) resistance 2 (mouse)	0.55	0.018
7999903	C16orf88	Chromosome 16 open reading frame 88	0.54	0.03
7923662	PIK3C2B	Phosphoinositide-3-kinase, class 2, beta polypeptide	0.54	0.0382
8049827	SEPT2	Septin 2	0.54	0.0236
8177277	RBMY1A1	RNA binding motif protein, Y-linked, family 1, member A1	0.53	0.0394
7956159	RPL41	Ribosomal protein L41	0.53	0.0344
8018196	CD300LF	CD300 molecule-like family member f	0.52	0.027
8100318	SGCB	Sarcoglycan, beta (43kDa dystrophin-associated glycoprotein)	0.52	0.0202
8013450	LGALS9B	Lectin, galactoside-binding, soluble, 9B	0.51	0.0258
8071301	C22orf25	Chromosome 22 open reading frame 25	0.51	0.0337
8065537	LOC100134868	Hypothetical LOC100134868	-0.5	0.0378
7986569	HERC2P2	Hect domain and RLD 2 pseudogene 2	-0.5	0.0494
8044236	GCC2	GRIP and coiled-coil domain containing 2	-0.51	0.0148
7932041	UPF2	UPF2 regulator of nonsense transcripts homolog (yeast)	-0.51	0.0263
8010967	NXN	Nucleoredoxin	-0.51	0.0129
7969153	TRIM13	Tripartite motif-containing 13	-0.52	0.0053
8093858	STK32B	Serine/threonine kinase 32B	-0.52	0.0113
8049544	LRRFIP1	Leucine rich repeat (in FLII) interacting protein 1	-0.52	0.0214
8149749	TNFRSF10D	Tumor necrosis factor receptor superfamily, member 10d, decoy with truncated death domain	-0.52	0.0106
8023063	ATP5A1	ATP synthase, H+ transporting, mitochondrial F1 complex, alpha subunit 1, cardiac muscle	-0.52	0.0052
8021365	ATP8B1	ATPase, aminophospholipid transporter, class I, type 8B, member 1	-0.53	0.0253
7958620	IFT81	Intraflagellar transport 81 homolog (Chlamydomonas)	-0.53	0.0283
8100026	ATP8A1	ATPase, aminophospholipid transporter (APLT), class I, type 8A, member 1	-0.53	0.0138
7961983	TM7SF3	Transmembrane 7 superfamily member 3	-0.54	0.0222
7903092	FNBP1L	Formin binding protein 1-like	-0.54	0.0416
8022251	PPP4R1	Protein phosphatase 4, regulatory subunit 1	-0.54	0.0361
7949645	ZDHHC24	Zinc finger, DHHC-type containing 24	-0.54	0.011
8029273	MEGF8	Multiple EGF-like-domains 8	-0.54	0.0268
8130032	FBXO30	F-box protein 30	-0.54	0.0122
8129953	HIVEP2	Human immunodeficiency virus type I enhancer binding protein 2	-0.54	0.0167
7915612	PTCH2	Patched homolog 2 (Drosophila)	-0.55	0.0398
7919269	RNU1-1	RNA, U1 small nuclear 1	-0.56	0.0263
8021914	ADNP2	ADNP homeobox 2	-0.56	0.0401
8021113	C18orf25	Chromosome 18 open reading frame 25	-0.56	0.0121
8020308	C18orf1	Chromosome 18 open reading frame 1	-0.56	0.0255
7913883	PAFAH2	Platelet-activating factor acetylhydrolase 2, 40kDa	-0.56	0.0438
8103389	CTSO	Cathepsin O	-0.56	0.0474
8020323	RNMT	RNA (guanine-7-) methyltransferase	-0.56	0.0162
8026300	CD97	CD97 molecule	-0.57	0.0173
8010454	RNF213	Ring finger protein 213	-0.57	0.0109
8167013	PHF16	PHD finger protein 16	-0.57	0.0303
7952436	ESAM	Endothelial cell adhesion molecule	-0.57	0.0246
7909745	KCTD3	Potassium channel tetramerisation domain containing 3	-0.57	0.0435
7951133	MAML2	Mastermind-like 2 (Drosophila)	-0.57	0.018
7966878	CIT	Citron (rho-interacting, serine/threonine kinase 21)	-0.58	0.0094
7899436	SESN2	Sestrin 2	-0.58	0.0098
8006531	SLFN5	Schlafen family member 5	-0.59	0.0221
8023561	LMAN1	Lectin, mannose-binding, 1	-0.59	0.0458
8144378	AGPAT5	1-acylglycerol-3-phosphate O-acyltransferase 5	-0.6	0.0263

7902227	GADD45A	Growth arrest and DNA-damage-inducible, alpha	-0.6	0.0322
7902553	IFI44	Interferon-induced protein 44	-0.6	0.0227
8115851	STC2	Stanniocalcin 2	-0.6	0.002
8050007	PXDN	Peroxidasin homolog (Drosophila)	-0.6	0.011
8129418	PTPRK	Protein tyrosine phosphatase, receptor type, K	-0.6	0.0363
7972217	SPRY2	Sprouty homolog 2 (Drosophila)	-0.61	0.0216
8165794	CD99	CD99 molecule	-0.61	0.0087
8021727	CNDP2	CNDP dipeptidase 2 (metallopeptidase M20 family)	-0.61	0.0355
7934906	ACTA2	Actin, alpha 2, smooth muscle, aorta	-0.61	0.0379
8023195	SMAD2	SMAD family member 2	-0.61	0.0374
7927732	ARID5B	AT rich interactive domain 5B (MRF1-like)	-0.61	0.0465
8111524	UGT3A2	UDP glycosyltransferase 3 family, polypeptide A2	-0.62	0.0164
8113790	39143	Membrane-associated ring finger (C3HC4) 3	-0.62	0.0192
7967028	RNU4-2	RNA, U4 small nuclear 2	-0.62	0.0344
8105340	GZMA	Granzyme A (granzyme 1, cytotoxic T-lymphocyte-associated serine esterase 3)	-0.62	0.0169
7972579	TMTC4	Transmembrane and tetratricopeptide repeat containing 4	-0.62	0.0258
8177426	DAZ2	Deleted in azoospermia 2	-0.62	0.0061
8022882	ZNF24	Zinc finger protein 24	-0.62	0.0279
8004416	CHRNB1	Cholinergic receptor, nicotinic, beta 1 (muscle)	-0.63	0.028
8023415	TCF4	Transcription factor 4	-0.63	0.0273
7987439	GPR176	G protein-coupled receptor 176	-0.63	0.0131
8020527	C18orf8	Chromosome 18 open reading frame 8	-0.63	0.0226
7972713	EFNB2	Ephrin-B2	-0.64	0.0219
8020267	CEP192	Centrosomal protein 192kDa	-0.66	0.0224
8023377	MEX3C	Mex-3 homolog C (C. elegans)	-0.67	0.0276
7969574	MIR622	microRNA 622	-0.67	0.0006
7925876	PFKP	Phosphofructokinase, platelet	-0.68	0.0115
8094911	ATP10D	ATPase, class V, type 10D	-0.68	0.0489
7988789	DMXL2	Dmx-like 2	-0.69	0.0129
8023261	ACAA2	Acetyl-CoA acyltransferase 2	-0.69	0.0109
8070182	RCAN1	Regulator of calcineurin 1	-0.7	0.0359
8019857	NDC80	NDC80 homolog, kinetochore complex component (S. cerevisiae)	-0.7	0.0465
8023766	RTTN	Rotatin	-0.7	0.0186
8071134	C22orf37	Chromosome 22 open reading frame 37	-0.71	0.049
8102247	LOC285456	Hypothetical LOC285456	-0.71	0.0219
8002403	MTSS1L	Metastasis suppressor 1-like	-0.71	0.0201
8176878	DAZ1	Deleted in azoospermia 1	-0.71	0.0171
7948775	C11orf48	Chromosome 11 open reading frame 48	-0.72	0.0397
7969166	KCNRG	Potassium channel regulator	-0.72	0.007
7982868	CHAC1	ChaC, cation transport regulator homolog 1 (E. coli)	-0.72	0.0265
8158372	SET	SET nuclear oncogene	-0.73	0.0123
8049448	AGAP1	ArfGAP with GTPase domain, ankyrin repeat and PH domain 1	-0.73	0.0397
8124391	HIST1H2AB	Histone cluster 1, H2ab	-0.73	0.0171
7988444	MYEF2	Myelin expression factor 2	-0.74	0.0237
8102800	SLC7A11	Solute carrier family 7, (cationic amino acid transporter, y+ system) member 11	-0.74	0.0002
8022441	ROCK1	Rho-associated, coiled-coil containing protein kinase 1	-0.75	0.0051
8021286	C18orf54	Chromosome 18 open reading frame 54	-0.76	0.0367
8023871	ZADH2	Zinc binding alcohol dehydrogenase domain containing 2	-0.77	0.0143
8113358	ST8SIA4	ST8 alpha-N-acetyl-neuraminide alpha-2,8-sialyltransferase 4	-0.78	0.0083
8106986	RHOBTB3	Rho-related BTB domain containing 3	-0.78	0.0153
7923453	KDM5B	Lysine (K)-specific demethylase 5B	-0.79	0.0066
7943160	SCARNA9	Small Cajal body-specific RNA 9	-0.8	0.0356
8111136	FAM134B	Family with sequence similarity 134, member B	-0.81	0.0288

73

8130176	ULBP3	UL16 binding protein 3	-0.81	0.0429
8100362	LNX1	Ligand of numb-protein X 1	-0.82	0.0233
8027002	GDF15	Growth differentiation factor 15	-0.82	0.0041
8088958	GBE1	Glucan (1,4-alpha-), branching enzyme 1	-0.84	0.0367
8095854	SEPT11	Septin 11	-0.84	0.0401
8020100	RALBP1	RalA binding protein 1	-0.84	0.0133
7902594	PRKACB	Protein kinase, cAMP-dependent, catalytic, beta	-0.86	0.0071
7981824	CYFIP1	Cytoplasmic FMR1 interacting protein 1	-0.86	0.0245
8114572	HBEGF	Heparin-binding EGF-like growth factor	-0.87	0.0026
7988876	MYO5C	Myosin VC	-0.88	0.0189
8163452	FKBP15	FK506 binding protein 15, 133kDa	-0.88	0.0009
7981990	SNORD116-21	Small nucleolar RNA, C/D box 116-21	-0.89	0.011
8119088	CDKN1A	Cyclin-dependent kinase inhibitor 1A (p21, Cip1)	-0.89	0.0049
8107100	RGMB	RGM domain family, member B	-0.91	0.0319
8171758	SCARNA9L	Small Cajal body-specific RNA 9-like (retrotransposed)	-0.91	0.0178
8023646	BCL2	B-cell CLL/lymphoma 2	-0.92	0.0028
8057056	TTN	Titin	-0.92	0.0013
8116998	JARID2	Jumonji, AT rich interactive domain 2	-0.92	0.0085
7964834	CPM	Carboxypeptidase M	-0.94	0.0308
7915592	RNU5D	RNA, U5D small nuclear // RNA, U5D small nuclear	-0.94	0.0096
7971565	LPAR6	Lysophosphatidic acid receptor 6	-0.96	0.0334
8081564	CD96	CD96 molecule	-0.96	0.0041
8056877	CHRNA1	Cholinergic receptor, nicotinic, alpha 1 (muscle)	-0.96	0.0025
8174361	TSC22D3	TSC22 domain family, member 3	-0.97	0.0005
8134122	AKAP9	A kinase (PRKA) anchor protein (yotiao) 9	-0.99	0.0023
8142554	AASS	Aminoadipate-semialdehyde synthase	-1.01	0.0055
8030946	ZNF808	Zinc finger protein 808	-1.02	0.0037
8021470	PMAIP1	Phorbol-12-myristate-13-acetate-induced protein 1	-1.02	0.002
8133938	CROT	Carnitine O-octanoyltransferase	-1.04	0.0121
7970975	SOHLH2	Spermatogenesis and oogenesis specific basic helix-loop-helix 2	-1.04	0.0047
8072735	APOL1	Apolipoprotein L, 1	-1.06	0.01
8021183	SCARNA17	Small Cajal body-specific RNA 17	-1.06	0.0077
8022531	NPC1	Niemann-Pick disease, type C1	-1.09	0.0119
7997048	DDX19B	DEAD (Asp-Glu-Ala-As) box polypeptide 19B	-1.13	0.0249
8028311	SPINT2	Serine peptidase inhibitor, Kunitz type, 2	-1.15	0
8058512	PLEKHM3	Pleckstrin homology domain containing, family M, member 3	-1.16	0.0029
7929574	**DNTT**	**Deoxynucleotidyltransferase, terminal**	**-1.16**	**0.0087**
8020423	MIB1	Mindbomb homolog 1 (Drosophila)	-1.17	0.0054
8004184	XAF1	XIAP associated factor 1	-1.18	0.0001
7922717	RGS16	Regulator of G-protein signaling 16	-1.22	0.0092
8095080	**PDGFRA**	**Platelet-derived growth factor receptor, alpha polypeptide**	**-1.33**	**0.0028**
8103906	MGC24125	Hypothetical protein MGC24125	-1.34	0.0035
7978712	CLEC14A	C-type lectin domain family 14, member A	-1.41	0.0021
8020110	RAB31	RAB31, member RAS oncogene family	-1.42	0.0053
8105331	GZMK	Granzyme K (granzyme 3; tryptase II)	-1.43	0.0029
8091600	PLCH1	Phospholipase C, eta 1	-1.45	0.0247
7964460	**DDIT3**	**DNA-damage-inducible transcript 3**	**-1.47**	**0.0088**
7926677	OTUD1	OTU domain containing 1	-1.63	0.0018
8088560	ADAMTS9	ADAM metallopeptidase with thrombospondin type 1 motif, 9	-1.78	0.001
8019988	PTPRM	Protein tyrosine phosphatase, receptor type, M	-2.51	0

8.1.2 Supplementary Table 2. List of downregulated genes in primary childhood ALL responding well to glucocorticoids and downregulated genes after MondoA knockdown in Nalm6 cells of the current study.

Gene symbol	Description	Related function
ACAA2	Acetyl-CoA acyltransferase 2	Mitochondrial fatty acid beta-oxidation
BCL2	B-cell CLL/lymphoma 2	Anti-apoptosis
CD99	CD99	Apoptosis
CYFIP1	Cytoplasmic FMR1 interacting protein 1	Regulation of cell shape
DNTT	Deoxynucleotidyltransferase, terminal	Lymphocyte differentiation
GBE1	Glucan (1,4-alpha-), branching enzyme 1	Glucose metabolism
KCTD3	Potassium channel tetramerisation domain containing 3	Voltage-gated potassium channel activity
MYO5C	Myosin VC	Granule trafficking
PHF16	PHD finger protein 16	Histone modification
PXDN	Peroxidasin homolog (Drosophila)	Extracellular matrix association
RCAN1	Regulator of calcineurin 1	Inhibitor of calcineurin-dependent signaling
SEPT11	Septin 11	Cytokinesis and vesicle trafficking
SET	SET nuclear oncogene	Anti-apoptosis and histone modification
STK32B	Serine/threonine kinase 32B	ND

8.1.3 Supplementary Table 3. Patient data of Figure 5 A and Figure 12

This table was modified after the dissertation by Dr. Uwe E. Hattenhorst with kind permission of the author (Uwe E. Hattenhorst, 2003) .

Patient ID	Age	Sex	Translocations	Risk group	MondoA expression	Leukocytes day 0
ALL25HCS	4.4	M		1	7915,7	50000
ALL31ARB	7.7	F		2	12856,2	77400
ALL33LUM	2.5	F		2	7338,2	2100
ALL34REH	5.1	F	TEL-AML1	1	7026,4	38800
ALL36IHP	2.9	M		2	2566,7	11600
ALL37UEH	0.6	F	MLL-X	3	1897,7	n.s.
ALL38IER	4.3	M		2	4045,2	8600
ALL39AHS	4.4	M	TEL-AML1	1	6422,2	22600
ALL40EEL	3.4	M		1	5744,2	33900
ALL41APS	4.3	M		2	3707,4	6500
ALL42ORK	5.7	M		1	7305,5	2800
ALL43MED	3	F	TEL-AML1	2	7497,5	3700
ALL45NUK	11.8	F		2	3643,5	2000
ALL46ROY	2.1	F		1	7458,4	87200
ALL47HEM	5.6	M		3	4205,4	14500
ALL48PIL	9.9	M		2	5914,6	134000
ALL49ERD	11	M		3	4929,4	16700
ALL50GAJ	4	F	TEL-AML1	1	6065,4	1700
ALL51ERT	15.2	F		2	3208,7	8900
ALL52HCS	14.9	F		2	6363,6	57500
ALL53TAB	4.1	F		1	4354,4	4800
ALL54TEY	3.5	M		1	6571,0	56700
ALL55ZAB	8.11	F	TEL-AML1	1	7529,5	2100
ALL56WET	4.11	F		2	4065,2	39000
ALL57SUN	10.6	M		2	4476,3	443400

Age at time of diagnosis (year, months). M male, F female. Assignation to risk group after GPOH. Relative MondoA expression to FEB cells (see Figure 5 A). Leukocytes day 0: Leukocytes in cells/μL in the peripheral blood at time of diagnosis. n.s. not specified

8.1.4 Supplementary Table 4. Raw data of the metabolomic analysis via mass spectrometry in cooperation with the Helmholtz Center Munich.

Intracellular amount of glycerophospholipids, acylcarnitines, aminoacids, sphingolipids and sugars in pSInegative and pSImondoA cells.

Class	pSInegative#1	pSInegative#2	pSImondoA#1	pSImondoA#2
glycerophospholipids	0.61	0.657	0.763	0.787
glycerophospholipids	0.302	0.278	0.197	0.223
glycerophospholipids	0.169	0.177	0.108	0.131
glycerophospholipids	0.022	0.019	0.024	0.028
glycerophospholipids	0.05	0.05	0.076	0.046
glycerophospholipids	2	1.6	1.12	1.49
glycerophospholipids	0.232	0.195	0.244	0.294
glycerophospholipids	0.039	0.044	0.052	0.061
glycerophospholipids	0.009	0.011	0.01	0.015
glycerophospholipids	0.115	0.111	0.126	0.127
glycerophospholipids	0.367	0.425	0.317	0.316
glycerophospholipids	0.916	0.906	0.533	0.768
glycerophospholipids	0.545	0.512	0.349	0.423
glycerophospholipids	0.507	0.417	0.282	0.37
glycerophospholipids	0.467	0.371	0.302	0.328
glycerophospholipids	0.342	0.511	0.519	0.544
glycerophospholipids	0.101	0.115	0.072	0.094
glycerophospholipids	0.009	0.011	0.013	0.014
glycerophospholipids	0.108	0.104	0.184	0.093
glycerophospholipids	0.068	0.103	0.13	0.092
ac.carnitines	0.025	0.026	0.02	0.02
ac.carnitines	0.001	0.002	0.002	0.002
aminoacids	2.02	1.5	1.91	2.49
sphingolipids	0.085	0.089	0.053	0.061
sphingolipids	0.114	0.118	0.098	0.101
sphingolipids	0.098	0.125	0.091	0.083
sphingolipids	0.048	0.061	0.04	0.042
sphingolipids	0.02	0.017	0.013	0.014
sphingolipids	2.29	2.63	1.8	2.03
sphingolipids	0.176	0.21	0.156	0.152
sphingolipids	0.174	0.194	0.138	0.144
sphingolipids	0.046	0.056	0.036	0.036
sphingolipids	0.323	0.365	0.235	0.278
sphingolipids	0.353	0.433	0.253	0.327
sphingolipids	0.004	0.001	0.006	0.002
sphingolipids	0.009	0.012	0.001	0.009
sugars	9.21	7.03	6.87	3.08

Danksagung

An dieser Stelle möchte ich meinem Betreuer Herrn Dr. med. PhD Thomas Grünewald (Leiter der AG Grünewald am pathologischen Institut der LMU München) für seine sehr hilfreiche und engagierte Betreuung im Labor und seine sachkundige Beratung beim Erstellen der Publikationen ganz herzlich danken. Herrn PD Dr. rer. nat. Günther Richter (Leiter des Labors für funktionelle Genomik und Transplantationsbiologie/Children's Cancer Research Center der Kinderklinik Schwabing) danke ich für seine Beratung bei methodischen Fragestellungen und insbesondere bei der Analyse der Microarraydaten. Herrn Prof. Dr. Stefan Burdach (Direktor der Kinderklinik Schwabing der Technischen Universität München) danke ich sehr für die freundliche Überlassung dieser Doktorarbeit, für die hilfreichen Anregungen und für seine gutachterliche Stellungnahme. Frau Prof. Dr. Gisela Keller (Leiterin der AG Keller, Institut für Pathologie des Klinikums rechts der Isar) und Frau Prof. Dr. Angela Krackhardt (Leiterin der AG Krackhardt, III. Medizinische Klinik des Klinikums rechts der Isar) möchte ich ebenfalls für ihre gutachterlichen Stellungnahmen danken. Ich danke auch der technischen Assistentin Colette Zobywalski für ihre zuverlässige Unterstützung und meinen Laborkollegen Uwe Thiel, Kristina Hauer, Stephanie Plehm, Isabella Miller und Franziska Blaeschke für die methodischen Ratschläge und die gute Zusammenarbeit. Ganz besonders danken möchte ich Christoph Kunzer und meiner Familie für die ausdauernde Unterstützung insbesondere während der Erstellung dieser Doktorarbeit.

Curriculum vitae

Caroline Magdalena Wernicke, geb. am 13.05.1987 in Herbolzheim

SCHULE/STUDIUM

09/1997 – 07/2006	Gymnasium Kenzingen, Abschluss: **Abitur 07/2006**, Note: 1.0
09/2006 – 09/2008	Humanmedizin (Vorklinik) an der Albert-Ludwigs-Universität Freiburg, **1. Abschnitt der ärztlichen Prüfung 09/2008**, Note: sehr gut
09/2008 – 10/2013	Humanmedizin (Klinik) an der Technischen Universität München, **2. Abschnitt der ärztlichen Prüfung 10/2013**, Note: sehr gut
08/2009 – 07/2010	Erasmus Auslandsstudium an der Universität Nizza, Frankreich
08/2011 – 09/2011	Famulatur in der chirurgischen Notaufnahme am Hospital Universitario del Valle, Cali, Kolumbien
04 – 07/2012	PJ-Tertial Chirurgie in der Allgemein- und Neurochirurgie am Hospital Fernandez in Buenos Aires, Argentinien
08 – 11/2012	PJ-Tertial Innere Medizin in der Hämatologie und der Pulmonologie/Intensivmedizin am New York Presbyterian Hospital in New York und in der Inneren Medizin und in der Gastroenterologie am Methodist Hospital in Houston, Texas
12/2012 – 03/2013	PJ-Wahltertial Pädiatrie am Kantonspital in Winterthur, Schweiz
Seit 01/2014	**Assistenzärztin** an der Kinderklinik Schwabing, München

STIPENDIEN

- Stipendiatin der Studienstiftung des deutschen Volkes e.V.
- Stipendium für das Austauschprogramm der TU München mit der Weill Cornell Medical School, New York/Houston
- Jahresstipendium des Deutschen Akademischen Austauschdienstes (DAAD) für die USA
- Promos - Stipendium des DAAD für Argentinien

Auflistung der Vorveröffentlichungen

Originalarbeiten:

Wernicke CM, Richter GH, Beinvogl BC, Plehm S, Schlitter AM, Bandapalli OR, Prazeres da Costa O, Hattenhorst UE, Volkmer I, Staege MS, Esposito I, Burdach S, Grunewald TG
Mondo A is highly overexpressed in acute lymphoblastic leukemia and modulates their metabolism, differentiation and survival
Leukemia Research 2012, 36(9):1185-92

Wernicke CM, Grunewald TG, Juenger H, Kuci S, Kuci Z, Koehl U, Mueller I, Doering M, Peters C, Lawitschka A, Kolb HJ, Bader P, Burdach S, von Luettichau I.
Mesenchymal stromal cells for treatment of steroid-refractory GvHD: a review oft he literature and two pediatric cases.
International Archives of Medicine 2011, Aug 15;4(1):27.doi: 10.1186/1755-7682-4-27.

Kongressbeiträge:

Wernicke CM, Grunewald TG, Juenger H, Kolb HJ, Burdach S, von Luettichau I
Postervortrag: „Effektive Therapie einer fulminanten GvHD der Lunge und der Haut durch third-party Transplantation humaner mesenchymaler Stromazellen"
106. Jahrestagung der deutschen Gesellschaft für Kinder- und Jugendmedizin (DGKJ), Potsdam, September 15-19 2010

A. Sipol, T. Grünewald, **C. Wernicke**, G. Richter, St. Burdach
„The metabolic stress sensor MLXIP mediates malignancy of cALL in vivo"
Acute Leukemias XV, Biology and Treatment strategies, Munich, February 22-25 2015

Alexandra Sipol, Thomas Grünewald, Guenther Richter, **Caroline Wernicke**, Hans-Jochem Kolb, Torsten Haferlach and Stefan Burdach
„Overexpression of the Metabolic Stress Sensor and Proglycolytic Transcription Factor MLXIP Mediates Malignancy of Common Acute Lymphoblastic Leukemia in Vivo and Is Targetable By Allorestricted Peptide Specific T Cells"
56 ASH Annual Meeting, San Francisco, December 6-9 2014
ASH Abstract Achievement Award

Alexandra A. Sipol, Günther H.S. Richter, **Caroline M. Wernicke**, Thomas G.P. Grunewald, Stefan Burdach
„Overexpression of the pro-glycolytic transcription factor MondoA enhances malignant potential of ALL *in vivo"*
AACR Annual Meeting, San Diego, April 5-9 2014

Alexandra A. Sipol, Günther H.S. Richter, **Caroline M. Wernicke**, Thomas G.P. Grunewald, Boris V. Afanasiev and Stefan Burdach
„Overexpression of the pro-glycolytic transcription factor MondoA mediates malignancy of ALL in vivo"
VIIth Raisa Gorbacheva Memorial Meeting, Astana, Kazakhstan, 20-21 September 2013